

Submitted to  
manuscript

# Solving Inventory Management Problems with Inventory-dynamics-informed Neural Networks

Lucas Böttcher

Computational Social Science, Frankfurt School of Finance and Management, 60322 Frankfurt, Germany, l.boettcher@fs.de  
Dept. of Computational Medicine, UCLA, Los Angeles, CA 90095-1766, USA

Thomas Asikis

Computational Social Science, ETH Zurich, 8092 Zurich, Switzerland

Ioannis Fragkos

Dept. of Technology and Operations Management, Rotterdam School of Management, Erasmus University Rotterdam, 3062  
Rotterdam, Netherlands

**Problem definition:** A key challenge in inventory management is to identify policies that optimally replenish inventory from multiple suppliers. To solve such optimization problems, inventory managers need to decide what quantities to order from each supplier, given the on-hand inventory and outstanding orders, so that the expected backlogging, holding, and sourcing costs are jointly minimized. Inventory management problems have been studied extensively for over 60 years, and yet even basic dual sourcing problems, in which orders from an expensive supplier arrive faster than orders from a regular supplier, remain intractable in their general form. In addition, there is an emerging need to develop proactive, scalable optimization algorithms that can adjust their recommendations to dynamic demand shifts in a timely fashion.

**Methodology/results:** In this work, we approach dual sourcing from a neural-network-based optimization lens and incorporate inventory dynamics into the design of deep neural networks. We show that the proposed inventory-dynamics-informed neural networks (IDINNs) are able to learn near-optimal policies of commonly used instances within a few minutes of CPU time on a regular personal computer. To demonstrate the versatility of IDINNs, we also show that they can control inventory dynamics with empirical, non-stationary demand distributions that are challenging to tackle effectively using alternative, state-of-the-art approaches.

**Managerial implications:** Our work shows that high-quality solutions of complex inventory management problems with non-stationary demand can be obtained with deep neural-network optimization approaches that directly account for inventory dynamics in their optimization process. As such, our research opens up new ways of efficiently managing complex, high-dimensional inventory dynamics.

**Key words:** inventory management; sourcing strategies; optimal control; inventory-dynamics-informed neural networks

**History:** This paper is in preprint stage.

arXiv:2201.06126v3 [cs.LG] 7 Mar 2022

## 1. Introduction

Inventory management problems of various forms have been studied for more than six decades by the operations management and operations research communities. Progress in solving such problems has led to effective and efficient supply chains of unprecedented size and complexity. Despite some celebrated results, such as the optimality of base-stock policies in single-sourcing systems with backlogging (Scarf and Karlin 1958), most inventory management problems have such complex dynamics that finding optimal policies has been a major challenge. For example, in inventory management problems with two suppliers (*i.e.*, dual sourcing problems), the general structure of the optimal policy remains unknown after more than half a century of intense research (Sun and Van Mieghem 2019, Goldberg et al. 2021). Since dual sourcing and other inventory management problems are analytically intractable, a vast amount of effort has been put into designing heuristics that guide effective order decisions.

In this work, we study dual sourcing in its classic form, as first analyzed by Barankin (1963) and Fukuda (1964), from a neural-network optimization lens. Starting from a direct optimization of the underlying inventory dynamics, we develop inventory management systems that are based on neural networks and we show that they are able to approximate the structure of optimal policies and outperform effective dual-sourcing heuristics in commonly used instances. We also show that the proposed neural-network optimization methods are able to effectively control complex inventory dynamics with demand distributions that are inferred from empirical data.

Using state-of-the-art machine learning methods combined with domain-specific knowledge is a relatively new and promising venue for inventory management research (Xin and Van Mieghem 2021, Song et al. 2020). An important contribution in this direction is the work by Gijsbrechts et al. (2020), who utilize deep reinforcement learning (RL)-based optimization to control three archetypal inventory management problems. The authors show that an actor-critic RL algorithm can deliver competitive performance against problem-specific heuristics. This is an important step towards the design of more generic algorithms that are able to solve a larger set of optimization problems with less restrictive assumptions. In this paper, we contribute to this line of research, and more generally to solving discrete stochastic optimization problems, by introducing inventory-dynamics-informed neural networks (IDINNs) that directly control dual sourcing dynamics by learning effective order policies.

The optimization methods that we develop in this article build on previous works that use automatic differentiation (Linnainmaa 1976, Paszke et al. 2017, Baydin et al. 2018) and dynamics-informed neural networks (Raissi et al. 2019) to solve complex control and optimization problems (Holl et al. 2020, Jin et al. 2020, Wang et al. 2020, Asikis et al. 2020, Böttcher et al. 2022). We construct neural networks that take both the current inventory and previous orders as inputs and

minimize the expected backlogging, holding, and sourcing costs. There are two major challenges that arise in training neural networks for inventory-dynamics control. First, the evolution of inventory dynamics is described by a stochastic dynamical system, so neural networks have to be trained on a sufficiently large number of realizations to learn effective and generalizable<sup>1</sup> order policies. Second, adjusting neural-network weights during training relies on propagating real-valued gradients, while neural-network outputs (*i.e.*, replenishment orders) are required to be integer-valued, because they influence the system transition to a new state. To solve such a discrete optimization problem with real-valued gradient-descent learning algorithms, we decouple parts of the neural-network output during training to recover real-valued gradients (Asikis 2021).

### 1.1. Contributions

In summary, our work contributes to the extant inventory management literature in the following aspects.

- We show that the proposed IDINNs are able to approximate optimal inventory management policies without any previous knowledge on their structure. In particular, our focus is not only on comparing the optimal objective values with the values obtained by the neural network, but also comparing the actual policies we derive against the optimal ones, when the latter ones are possible to compute. This form of comparison, although uncommon in the literature, sheds light on the structure of ordering policies and their resemblance to optimal ones. Consequently, we show evidence that neural networks are able to uncover policies that resemble the structure of optimal policies, instead of simply attaining near-optimal objective values with policies of arbitrary structure.
- Our approach is computationally attractive, since it requires only between a few seconds and a few minutes of CPU time on a regular personal computer. To the best of our knowledge, this is the first generic approach that can compete and even outperform the performance of tailored policies using a reasonable amount of computational power. A key technique behind such computational gains is fractional decoupling (Asikis 2021), a method that allows one to output discrete actions (*i.e.*, integer-valued quantities) and still adjust real-valued neural-network weights while optimizing the employed neural networks.
- Finally, we demonstrate the versatility of IDINNs by using them to effectively control instances of a dual-sourcing problem with empirically inferred, non-stationary demand distributions (Manary and Willems 2021). In the majority of simulated realizations, we find that IDINNs outperform a state-of-the-art inventory control heuristic.

<sup>1</sup>In the context of controlling stochastic dynamical systems, we refer to a neural-network-based control policy as “generalizable” if the learned policy, trained on specific realizations of the stochastic dynamics, is able to achieve similar performance (*e.g.*, a similar loss) on unseen realizations.

The remainder of this paper is organized as follows. Section 2 reviews previous work on inventory management problems, and discusses similarities and differences between IDINNs and other neural-network-based optimization methods. Section 3 formulates the generic problem of controlling discrete dynamic systems with neural networks, and Section 4 illustrates the methodology on a simple inventory model with backlogging, establishing a correspondence between the network architecture and the structure of the optimal solution of the mode. Then, we customize IDINNs to dual-sourcing problems in Section 5, and present computational experiments in a wide variety of instances in Section 6. Finally, we conclude our work in Section 7, reflecting on avenues for future research.

## 2. Literature Review

We next review some relevant work from the inventory management literature and the rapidly growing field of neural-network-based control and optimization.

### 2.1. Inventory Management with Dual Sourcing

Research in dual sourcing inventory management problems is vast and spans over more than five decades. The core problem where one can order from a cheaper but slower and a faster but more costly supplier using a dynamic order allocation rule was first studied by Barankin (1963) and Fukuda (1964), who showed that a single-index, dual-base-stock policy is optimal when the supplier lead times are one time period apart. When lead times differ more than one period, the optimal policy is state-dependent, as it depends on the vector of pipeline orders in a non-trivial way (Whittomere and Saunders 1977). As the difference between the supplier lead times grows larger, the problem becomes computationally intractable because of the associated “curse of dimensionality” (Powell 2007, Goldberg et al. 2021). Most of the literature has therefore focused on the development of heuristic policies, such as the single index (SI) (Scheller-Wolf et al. 2007), dual index (DI) (Veeraraghavan and Scheller-Wolf 2008), capped dual index (CDI) (Sun and Van Mieghem 2019), vector-base-stock (Sheopuri et al. 2010, Hua et al. 2015), (VBS) and tailored-based surge (TBS) (Allon and Van Mieghem 2010, Xin and Goldberg 2018, Chen and Shi 2019) policies.

Although the structure of optimal solutions remains unknown, some interesting properties have been derived. First, Sheopuri et al. (2010) observe that an inventory dynamics model with both a single supplier and lost sales can be derived as a special case of a dual sourcing system in which the fast supplier is able to deliver an order instantaneously, *after* the period’s demand has been realized. For appropriately chosen parameters, it is optimal to order from that supplier exactly as many items are necessary to clear the backlog, and therefore the corresponding ordering cost can be seen as a lost sales cost in a lost-sales model. The same authors observe that the state space can be compressed to  $l$  dimensions, where  $l$  is the lead time difference between the two suppliers,

and that, without loss of generality, the expedited supplier’s lead time can be set to zero when working in the compressed space. Second, following the analysis of Zipkin (2008b), Hua et al. (2015) characterize the structure of optimal solutions by showing that the value function is  $L^{\natural}$  convex. In particular, they show that regular orders are more sensitive to late-arriving orders than to earlier ones, while expedited orders are more sensitive to the imminent pipeline. Their result is used to construct a heuristic policy that performs very well against other approaches. In a subsequent study, Xin and Goldberg (2018) show that TBS is asymptotically optimal as the lead time of the regular supplier grows large and the lead time of the fast supplier remains fixed. Tailored-based surge is also near-optimal when demand comprises two components, a base distribution and a surge distribution, provided that the surge demand occurs with a small probability (Janakiraman et al. 2015). Finally, Sun and Van Mieghem (2019) show that CDI policies are robustly optimal, given demand that lies in a known polyhedral uncertainty set. The authors also establish that in the limiting case where the regular supplier’s lead time grows large and the lead time of the expedited supplier remains unchanged, CDI converges to TBS, thereby matching the main result of Xin and Goldberg (2018). Capped dual index policies achieve a good performance over a wide range of lead time differences and resemble DI policies for small lead time differences (Xin and Van Mieghem 2021), presumably because the effect of an additional parameter that describes order constraints (or “caps”) is negligible. Capped base-stock policies also exhibit good performance on single-sourcing, lost-sales inventory models (Xin 2021a,b). Adding a cap to a base-stock policy reduces the variance of ordered quantities, which may be advantageous in lost-sales models. Intuitively, while in backlogging systems an excessively large order can help clearing a large backlog, in lost-sales models it will only increase the inventory on hand and possibly the holding costs. This property of lost-sales models, namely the period “reset” of inventory to zero whenever demand is in excess, makes near-myopic and capping policies effective in practice (Morton 1971, Zipkin 2008a, Xin 2021b).

Dual sourcing can be extended in multiple other directions, such as having endogenous stochastic lead times (Song et al. 2017), multi-source systems (Song et al. 2021), non-stationary demand, and supplier capacities (Boute et al. 2021a). A comprehensive overview of dual-sourcing models is presented in Xin and Van Mieghem (2021), while Goldberg et al. (2021) provide a review of asymptotic analysis in inventory control problems and show how it can be applied to dual-sourcing models.

Our paper augments the above literature by offering an alternative perspective in modeling and controlling dual sourcing models, using inventory-dynamics-informed neural networks (IDINNs). To the best of our knowledge, ours is the first approach that shows how neural networks can compete with and even outperform inventory-management approaches developed after years of

specialized research on dual sourcing. From a methodological perspective, our paper is close to Gijbrecchts et al. (2020), who apply RL-based policy learning to a variety of inventory management problems. In particular, the authors show that the presented Asynchronous Advantage Actor-Critic (A3C) algorithm competes favorably with several known heuristics for lost-sales, dual-sourcing and multi-echelon models. The authors note that the initial tuning phase can be computationally burdensome. Evaluating one set of neural-network hyperparameters may take about 24 CPU hours. We build upon this research by using IDINNs that control the difference equations underlying inventory management dynamics with the help of fractional decoupling (Asikis 2021). When tested on datasets from the literature, our approach outperforms state-of-the-art dual-sourcing heuristics, using a few seconds up to a few minutes of CPU time on a regular personal computer. Our results provide evidence that the presented neural-network-based control methods are effective for solving dual-sourcing problems.

## 2.2. Neural-network-based Optimization and Control

The inventory-dynamics-informed neural networks (IDINNs) that we develop in this work to manage inventory replenishment have their origin in control theory and machine learning. In the context of inventory management, optimal control signals correspond to the orders that minimize the expected shortage, holding, and sourcing costs, given a certain state (*i.e.*, inventory and order pipeline). Such control approaches are connected to recent advances in automatic differentiation and physics-informed neural networks (Karniadakis et al. 2021, Raissi et al. 2019, Lutter et al. 2019, Zhong et al. 2020), which have found applications in modeling partially unknown systems (Roehrl et al. 2020). In physics-informed neural networks, one constrains the training process by including information on the spatio-temporal evolution of a physical system into the loss function. Such constraints are typically described by partial differential equations. In our work, the loss function is proportional to the expected total cost (*i.e.*, the expected sum of backlogging, holding, and sourcing costs over a certain time horizon) and we incorporate dynamic information in the training process by using the state variables of inventory dynamics (*i.e.*, on-hand inventory and pipeline orders) as inputs.

For deterministic, continuous-time dynamical systems with real-valued control signals, control frameworks that are based on neural ordinary differential equations (ODEs) were proposed by Asikis et al. (2020). In a related work by Böttcher et al. (2022), it has been shown that such neural ODE controllers are able to automatically learn control trajectories that resemble those of optimal control methods. Another work by Asikis (2021) extends the aforementioned framework with real-valued control signals to discrete action spaces. Here, we build on this discrete action-space formulation and study the ability of neural networks to control inventory dynamics with *stochastic* demand.

Designing neural-network-based control methods for discrete action spaces is challenging since standard neural-network optimization techniques rely on the learning of suitable *real-valued weights* based on the propagation of *real-valued gradients*. Chen et al. (2020) use neural event functions to model discrete and instantaneous changes in a continuous-time system. The work of Asikis (2021) introduces fractional decoupling to perform real-valued gradient calculations for control problems with discrete action spaces. Fractional decoupling calculates gradients based on real-valued variables, instead of using discrete values that are applied in the cost-function calculation of control problems with discrete action spaces. In this way, it is possible to use standard neural network optimization techniques and still generate discrete control signals (*e.g.*, discrete order quantities in inventory management problems). We describe further details about neural network architecture, optimizers, and learning dynamics in the e-companion.

Inventory-dynamics-informed neural networks have several advantages over model-free RL methods, which suffer from sample inefficiency resulting from underlying high-dimensional feature spaces (Jin et al. 2018). Reinforcement-learning algorithms are often based on learning target and behavior policies. The target policy is the policy or neural network that updates its own parameters. The behavior policy is the policy that samples trajectories and selects actions based on state observations.

In on-policy learning, the value function is learned from actions that are based on the current policy. In this case, behavior and target policies are the same. In off-policy learning, the value function is learned using different (*e.g.*, random) actions. Advantage Actor-Critic and other actor-critic algorithms are designed to be off-policy. Such off-policy algorithms are vulnerable to three error accumulation processes: (i) erroneous approximation of the target function (function approximation error), (ii) divergence of the target policy from the behavior policy (divergence error), and (iii) calculation of a value estimate by the target policy for an action-state pair based on value estimates of other action pairs (bootstrapping error). These three sources of error are known as the “deadly triad” of RL (Van Hasselt et al. 2018, Sutton and Barto 2018). By not using a value-based RL framework, we can avoid diverging and bootstrapping errors, two main challenges associated with the deadly triad. Since IDINNs are model-based and on-policy, they do not explicitly rely on value-function approximations obtained through randomly sampling trajectories. In addition, they do not explicitly use value estimates to derive their policy. Since the policies that IDINNs learn are used to generate future samples for learning, they do not suffer from the off-policy divergence problem.

To explain the main difference between IDINNs and RL-based optimization approaches, we briefly summarize their underlying structure and application areas. In RL, an *agent* performs a certain *action* in a surrounding *environment* (Sutton and Barto 2018). Actions are mapped to

a *reward*, which is used to determine an optimal action sequence for a given sequence of states. The ultimate goal is to solve an underlying optimization problem (*i.e.*, the Bellmann equation) iteratively using a Markov decision process. There are two major classes of RL algorithms: (i) model-free and (ii) model-based methods. The main difference between these two classes is that the former uses a trial-and-error approach in determining optimal actions, while the latter uses a model to describe interactions between agent and environment (Polydoros and Nalpanidis 2017). Model-free methods are widely used, but may converge slowly and entail the risk of exploring unfavorable actions ?. If an appropriate model can be used to explore the action space, model-based approaches may be a favorable alternative since they converge faster towards the desired solution that maximizes the reward function. Nevertheless, model-based approaches are often based on neural networks representing policy and value functions, and require a differentiable model that fully describes the environment, which might be challenging to derive for high dimensional or very complex control tasks ?.

If the deterministic or stochastic dynamics that describe a certain system are known, an alternative to RL-based approaches is to directly represent the state-action function by a single neural network and backpropagate gradients resulting from a gradient descent in the loss function. For inventory management problems, such as dual sourcing, the underlying dynamics can be formulated in terms of stochastic difference equations, and an inventory-dynamics-informed neural network can be constructed to learn the action in a particular state that minimizes the expected backlogging, holding, and sourcing costs.

To summarize, RL-based optimization is preferable in scenarios where the interactions between agent and environment cannot be fully characterized mathematically. If one wishes to optimize actions for controlling a known deterministic or stochastic dynamical system, it is more efficient to employ direct neural-network-based optimizations (Asikis et al. 2020, Böttcher et al. 2022).

### 3. Solving Discrete Stochastic Optimization Problems with Neural Networks

We consider discrete stochastic dynamics whose evolution is described by

$$s_{t+1} = f(s_t, a_t, D_t), \quad (1)$$

where  $s_t$  and  $a_t$  denote state and action variables at time  $t$ , respectively.  $D_t \sim \phi$  is a random variable, and  $f$  maps the current state, action, and realization of  $D_t$  to a new state  $s_{t+1}$ . Each state-action combination is associated with a cost  $c_t(s_t, a_t)$ . Our goal is to identify a policy  $\pi_t = \{a_{t+j} | j = 0, 1, \dots\}$  that minimizes the expected total cost over  $T$  periods

$$C_t^{(\pi_t)}(s_t, T) = \sum_{j=0}^T \gamma^j \mathbb{E}^{(\pi_t)} [c_{t+j}(s_{t+j}, a_{t+j})], \quad (2)$$

where  $\gamma \in (0, 1]$  is a discount factor and  $\mathbb{E}^{(\pi_t)} [c_{t+j}]$  is the expected cost at time  $t+j$  that results from policy  $\pi_t$ .

The long-run average expected cost of a policy  $\pi_t$ , which is independent of the initial state  $s_t$  when it exists, is defined as

$$J^{(\pi_t)} = \limsup_{T \rightarrow \infty} \left\{ \frac{1}{T} C_t^{(\pi_t)}(s_t, T) \right\}. \quad (3)$$

The objective of the discrete stochastic optimization problems that we are studying in this work is to identify the optimal policy  $\pi^*$  that yields the minimum expected cost per period over an infinite horizon, *i.e.*,  $\pi^* \in \arg \inf_{\pi_t} J^{(\pi_t)}$ .

Instead of pursuing a dynamic-programming approach, we parameterize policies using neural networks. Mathematically, a neural network is equivalent to a parametric family of multivariable, vector-valued functions. Specifically, a neural network represents the mapping  $F_{\mathbf{w}}: \mathcal{X} \subseteq \mathbb{R}^l \rightarrow \mathcal{Y} \subseteq \mathbb{R}^m$ , *i.e.*, mapping  $x = (x_1, \dots, x_l)^\top \in \mathcal{X}$  to  $y = F_{\mathbf{w}}(x) = (F_{\mathbf{w},1}(x), \dots, F_{\mathbf{w},m}(x))^\top \in \mathcal{Y}$  for a given value of the parameter  $\mathbf{w} \in \mathbb{R}^n$ . Note that an optimal, non-randomized policy associated with minimizing Eq. (3), also maps each state-space vector  $s$  to a corresponding action vector  $a$ . The focal problem of the neural-network control approach that we pursue in this work is therefore to determine the form of  $F_{\mathbf{w}}(\cdot)$  and to select the parameter  $\mathbf{w}$  so that (i)  $F_{\mathbf{w}}$  maps each state  $x$  to an action  $y = F_{\mathbf{w}}(x)$  and (ii) Eq. (3) is optimized. Theoretically, neural networks are able to represent such policies under mild conditions, as specified by universal approximation theorems (Hornik 1991, Hanin and Sellke 2017, Park et al. 2020). In practice, however, designing neural networks that represent optimal policies of discrete-time stochastic dynamical systems has been challenging (Gijsbrechts et al. 2020, Boute et al. 2021b). We next outline an algorithm that does so efficiently.

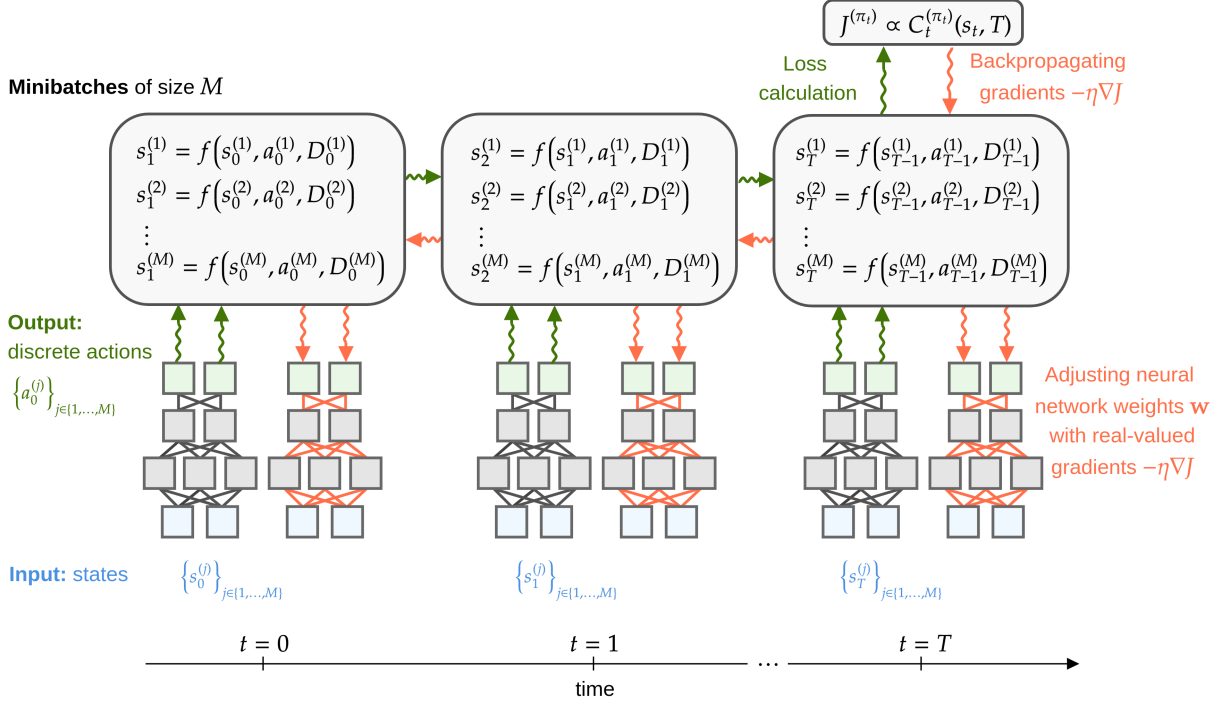
We denote neural-network policies and actions by  $\hat{\pi}_t$  and  $\hat{a}_t = \hat{a}_t(\mathbf{w})$ , respectively, which are functions with discrete outputs that depend on the neural network weights  $\mathbf{w}$ . Then, we approximate  $\mathbb{E}^{(\pi_t)}$  in Eq. (2) with  $\mathbb{E}^{(\hat{\pi}_t)}$ , using minibatches of size  $M$  and calculate

$$\mathbb{E}^{(\hat{\pi}_t)} [c_{t+j}(s_{t+j}, \hat{a}_{t+j})] = \frac{1}{M} \sum_{k=1}^M c_{t+j}(s_{t+j}^{(k)}, \hat{a}_{t+j}^{(k)}), \quad (4)$$

where  $s_t^{(k)}$  and  $\hat{a}_t^{(k)}$  denote state and neural-network actions in minibatch  $k$  at time  $t$ .

We optimize the neural network weights  $\mathbf{w}$  using RMSprop (Hinton 2016), which is an adaptive learning rate method that is well-suited to perform mini-batch weights updates (Kingma and Ba 2014). RMSprop uses the following update rules:

$$\begin{aligned} \mathbf{g}^{(n)} &= \nabla_{\mathbf{w}^{(n)}} J^{(\hat{\pi}_t)}, \\ v^{(n+1)} &= \alpha v^{(n)} + (1 - \alpha) [\mathbf{g}^{(n)}]^2, \\ \mathbf{w}^{(n+1)} &= \mathbf{w}^{(n)} - \frac{\eta}{\sqrt{v^{(n)} + \epsilon}} \mathbf{g}^{(n)}, \end{aligned} \quad (5)$$

**Figure 1** Schematic of solving discrete stochastic optimization problems with neural networks.

where  $n$  denotes the current training epoch,  $\eta$  is the learning rate,  $\alpha$  is a smoothing constant, and  $v$  is the weighted moving average of the squared gradient. The variable  $\epsilon$  is used to improve numerical stability of the gradient-descent weight updates. In our numerical experiments, we set  $\alpha = 0.99$  and  $\epsilon = 10^{-8}$ . Initially, the moving average of the squared gradient is  $v^{(0)} = 0$ .

A schematic of the described optimization process is shown in Figure 1. States  $\{s_t^{(j)}\}$  ( $1 \leq j \leq M$ ) are used as inputs in the neural network that learns actions that minimize the loss function  $J^{(\pi_t)}$ . Outputs of the neural network represent discrete actions  $\{\hat{a}_t^{(j)}\}$  ( $1 \leq j \leq M$ ), which we generate by subtracting the fractional part from the outputs of the last hidden layer (*i.e.*, the layer before the output layer). To backpropagate real-valued gradients and improve convergence, we detach this subtraction operation from the computational graph that is used for updating the weights of the neural network.

In the next section, we provide a motivating example that explains further details on the detachment (or “fractional decoupling”) approach and how the described optimization method can be utilized to learn the optimal order policy of single-sourcing problems.

#### 4. Motivating Example

Modern neural networks utilize several layers of activation functions to represent high-dimensional functions. One of the most commonly used activation function is the Rectified Linear Unit (ReLU), which returns the positive part of a real number, *i.e.*,  $\text{ReLU}(x) = \max\{0, x\}$  (Nair and Hinton 2010,

Schmidhuber 2015). This is in fact equivalent to the structure of base-stock policies, a class of policies that have been shown to be optimal for a variety of inventory control problems, including single-source problems with backlogged demand (Scarf and Karlin 1958), batch ordering (Veinott Jr 1965), multiple products under resource constraints (DeCroix and Arreola-Risa 1998), and Markov-modulated demand (Song and Zipkin 1993).

To illustrate how this connection can help IDINNs to effectively replenish inventory, we first focus on inventory management problems with a single supplier, whose optimal solutions can be viewed as special case of dual sourcing problems (see Sec. 5.1) for which the cost of the expedited supplier is too high for expedited orders to be placed. We explain the basic principles underlying IDINN-based inventory control, and show that such control approaches are indeed able to learn the optimal order policy of single sourcing problems.

For the mathematical formulation of the optimal order policy (Arrow et al. 1951, Scarf and Karlin 1958), we use  $l$  and  $z$  to respectively denote the replenishment lead time and the target inventory-position level (*i.e.*, the target level of inventory at hand plus all goods on order). The inventory position of single-sourcing dynamics at time  $t$  is

$$\tilde{I}_t = \begin{cases} I_t & \text{if } l = 0 \\ I_t + \sum_{i=1}^l q_{t-i} & \text{if } l > 0, \end{cases} \quad (6)$$

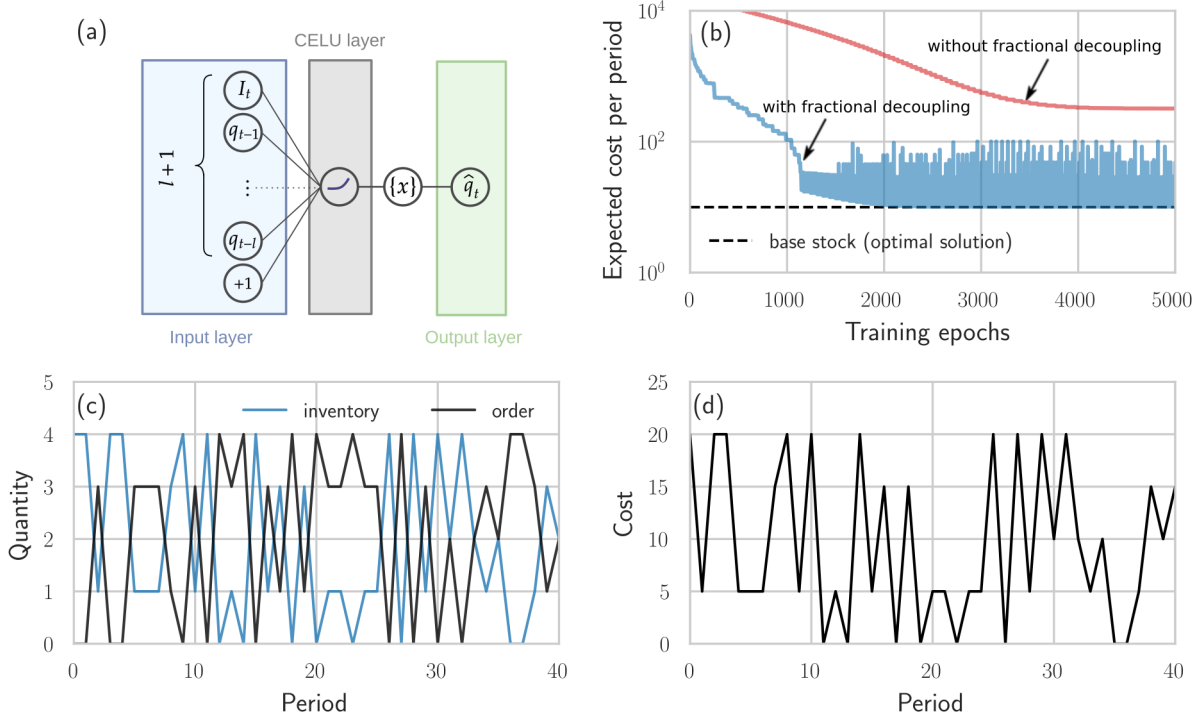
where  $q_t$  is the replenishment order placed at time  $t$ . We let  $b$  and  $h$  denote the unit backlogging and holding costs, respectively. The optimal target inventory level (Arrow et al. 1951) is given by the critical fractile

$$z^* = \Phi^{-1} \left( \frac{b}{b+h} \right), \quad (7)$$

where  $\Phi(x) = \Pr(D \leq x)$  denotes the cumulative distribution function of demand  $D$  during  $l+1$  periods. If the inventory position falls below  $z^*$  at time  $t$ , a replenishment order  $q_t = z^* - \tilde{I}_t$  is placed to bring the inventory position back to the optimal target level. The optimal single-sourcing policy (or “base stock”) is thus

$$q_t = [z^* - \tilde{I}_t]^+. \quad (8)$$

We observe that the optimal single-sourcing order policy is given by the positive part of  $z^* - \tilde{I}_t$ , which depends on the optimal inventory-position level  $z^*$ , the current net inventory, and the sum of previous orders  $q_{t-i}$  ( $0 \leq i \leq l$ ). To construct an IDINN, we use  $l+1$  inputs that represent the known net inventory and previous orders. We also include a bias term in the input layer to model the unknown optimal target inventory level  $z^*$ . All inputs are passed into an activation function that generalizes expression Eq. (8). Using a ReLU activation function will match exactly the structure of the optimal policy. However, while updating the weights of a ReLU activation using (5), it may end up in an inactive state in which it produces near-zero outputs (*e.g.*, due to a

**Figure 2** Controlling single-sourcing problems with inventory-dynamics-informed neural networks.

*Note.* (a) Schematic of an IDINN architecture for single-sourcing dynamics. The neural network uses as an input the  $(l + 1)$ -dimensional state  $s_t = (I_t, q_{t-1}, \dots, q_{t-l})$  and outputs an integer-valued action  $\hat{a}_t = \hat{q}_t$  after subtracting the fractional part  $\{[y_2]^+\}$  of the positive part of the CELU output  $[y_2]^+$  [see Eq. (11)]. In addition to  $s_t$ , the input layer also includes a bias term, indicated by a “+1”. The hidden layer is composed of a CELU activation. (b) Expected cost per period as a function of training epochs for  $h = 5$ ,  $b = 495$ ,  $l = 0$ ,  $T = 50$ , and demand distribution  $\mathcal{U}\{0, 4\}$ . The solid red line shows the expected cost evolution for training with a rounding layer a no fractional decoupling (no convergence towards the optimal solution). In all computations, we set  $\alpha = 1$  in the CELU activation. (c) Inventory and order quantity evolution, for an optimal base stock level of four units. (d) Cost evolution.

large negative bias term) (Douglas and Yu 2018). Once a ReLU reached such a state, it is unlikely to recover because corresponding gradients almost vanish and gradient-descent learning will not be able to substantially alter the weights; hence, the output will stay close to zero. We avoid this so-called “dead ReLU” problem by using a continuously differentiable exponential linear unit

$$\text{CELU}(x, \alpha) = [x]^+ - [\alpha(1 - \exp(x/\alpha))]^+, \quad (9)$$

which approaches  $\text{ReLU} = [x]^+$  in the limit  $\alpha \rightarrow 0^+$  (Barron 2017). An advantage of CELUs over ReLUs is that they are continuously differentiable, facilitating the gradient calculation in neural-network parameter optimization.

Figure 2(a) shows a schematic of the neural-network architecture that we use to learn the optimal single-sourcing policy. We denote the input vector and the output of the linear input layer by  $\mathbf{x} = [I_t, q_{t-1}, \dots, q_{t-l}]^\top \in \mathbb{R}^{(l+1) \times 1}$  and  $\mathbf{y}_1 = A_1 \mathbf{x} + \mathbf{b}_1$ , respectively. The second layer consists of a

single CELU activation function, so the bias term  $\mathbf{b}_1$  of the first layer is a scalar  $b_1 \in \mathbb{R}$  and the corresponding weight matrix  $A_1$  is a row vector  $[w_{1,1}, w_{1,2}, \dots, w_{1,l+1}] \in \mathbb{R}^{1 \times (l+1)}$  that contains the weights  $w_{1,j}$  ( $1 \leq j \leq l+1$ ). The quantity  $\mathbf{y}_1$  is passed into the CELU activation function that outputs

$$\mathbf{y}_2 = A_2 \mathbf{y}_1 + \mathbf{b}_2, \quad (10)$$

where  $A_2$  and  $\mathbf{b}_2$  denote the weight matrix and bias term of the second layer, respectively. In single-sourcing problems, the output of the neural network is a single order quantity; hence,  $\mathbf{y}_2$  is a scalar which we denote by  $y_2 \in \mathbb{R}$ . To obtain positive integer-valued order quantities  $\hat{q}_t \in \mathbb{N}_{\geq 0}$ , we subtract from the positive part of the CELU output  $[y_2]^+$  its fractional part  $\{[y_2]^+\}$ . That is,

$$\hat{q}_t = [y_2]^+ - \{[y_2]^+\}, \quad (11)$$

where  $\{x\} = x - \lfloor x \rfloor$  if  $x > 0$  and  $\lfloor \cdot \rfloor$  denotes the floor function. While updating neural-network weights by backpropagating gradients (Rumelhart et al. 1986), we detach the fractional part  $\{[y_2]^+\}$  from the computational graph. We will explain this step in more detail in the following paragraph.

To train the described neural network using backpropagation (Rumelhart et al. 1986), we minimize the expected total cost (4). We identify  $\mathbb{E}^{(\hat{\pi}_t)}[c_{t+j}]$  with the expected total cost at time  $t+j$  that results from the neural-network-based policy  $\hat{\pi}_t$ . In our simulations, we set the discount factor  $\gamma = 1$  and use a minibatch of  $M = 128$  demand realizations. To effectively adjust weights and biases, we employ fractional decoupling (Asikis 2021) that uses the real-valued positive part of the CELU output  $[y_2]^+$  and not the neural-network output  $\hat{q}_t = [y_2]^+ - \{[y_2]^+\}$  in the gradient backpropagation. This can be achieved by detaching  $\{[y_2]^+\}$  from the computational graph that is used to evaluate gradients. This method allows us to fine-tune real-valued neural-network weights and biases using real-valued gradients, even if the neural-network output  $\hat{q}_t$  is integer valued. Without fractional decoupling, loss functions and gradients are based on differences of two integers, reducing the possible update directions of gradient descent.

For a concrete example that illustrates how IDINNs approximate the optimal base-stock policy (8) over a training time horizon of  $T = 50$ , we set  $h = 5$ ,  $b = 495$ ,  $l = 0$ , and we use a uniform demand distribution  $\mathcal{U}\{0, 4\}$ . In this example, there is only one input and weight in the first layer (*i.e.*,  $x = I_t$  and  $A_1 = w_1$ ). We represent the optimal inventory position  $z^*$  in Eq. (8) by a bias term  $b_2$  in the CELU layer. The outputs of the first and second layers are

$$y_1 = w_1 x \quad (12)$$

$$y_2 = w_2 \text{CELU}(y_1 + b_2, \alpha), \quad (13)$$

respectively. To obtain a minimum-size representation of (8), we do not include a bias term in the output layer. The overall output of the neural network is given by Eq. (11).

For the given parameters, the optimal inventory level is  $z^* = 4$  and the corresponding optimal average cost per period is  $h(z^* - \bar{D}) = 10$ , where  $\bar{D} = 2$  is the mean demand. We find that the employed IDINN approaches the average cost level of the optimal base-stock policy after about 3,000 training epochs [solid blue line in Figure 2(b)]. The total training time is about 1.5 minutes on a regular personal computer. While approaching the optimal solution, small changes of the neural-network weights may entail large changes in the average cost, leading to the onset of oscillatory behavior of the average cost after about 3,000 training epochs. If we add a rounding layer instead of using fractional decoupling, the neural network does not reach the optimal base-stock cost due to the reduced set of possible gradient-descent directions [solid red line in Figure 2(b)].

After training, we selected the best model and extracted the weight and bias values. We find that  $w_1 = -0.5328$ ,  $b_1 = 2.1352$ , and  $w_2 = 1.8739$ . Observe that the IDINN approximates the optimal base-stock policy (8) since  $-b_1/w_1 \approx 4 = z^*$  and  $-w_2w_1 \approx 1$ . Figures 2(c,d) show that the IDINN we use in this example learned to produce order, inventory, and cost profiles that resemble those of an optimal base-stock policy with constant inventory position.

## 5. Managing Dual Sourcing Problems with Inventory-dynamics-informed Neural Networks

After having described the basic mechanisms of IDINNs in the context of inventory dynamics with a single supplier, we will now focus on dual-sourcing dynamics as a more complex example of inventory-management problems.

### 5.1. Dual Sourcing Model

We consider a dual-sourcing inventory control problem with stochastic demand. The first sourcing option is a “regular” supplier, R, that delivers goods with an integer lead time  $l_r > 0$  at a cost  $c_r$ . Goods can also be ordered from a second “emergency” supplier, E, with a shorter (non-negative) integer lead time  $l_e < l_r$  at a higher cost  $c_e > c_r$ . The premium for the expedited delivery through supplier E is thus  $c := c_e - c_r > 0$ .

We use  $I_t$  to denote the inventory-on-hand at the beginning of period  $t \in \{1, 2, \dots\}$ . The corresponding replenishment orders placed to suppliers E and R in period  $t$  are  $q_t^e$  and  $q_t^r$ , respectively. In each period  $t$ , the demand  $D_t$  is i.i.d. distributed according to a distribution function  $\phi$  with finite mean  $\mu$ .

Using these definitions, the sequence of events in each period of the dual-sourcing model are as follows.

1. At the beginning of period  $t$ , the inventory manager places replenishment orders  $q_t^r$  and  $q_t^e$  based on the last-observed net inventory,  $I_t$ , and the replenishment orders that have not arrived yet,  $Q_t^r = (q_{t-l_r}^r, \dots, q_{t-1}^r)$  and  $Q_t^e = (q_{t-l_e}^e, \dots, q_{t-1}^e)$ .

2. Orders  $q_{t-l_r}^r$  and  $q_{t-l_e}^e$  arrive and are added to the current inventory.

3. The demand  $D_t \sim \phi$  is revealed and subtracted from the current inventory.

Hence, the inventory (with backlogged excess demand) evolves according to

$$I_{t+1} = I_t + q_{t-l_r}^r + q_{t-l_e}^e - D_t. \quad (14)$$

The dual sourcing problem is a Markov decision process with state  $s_t = (I_t, Q_t^r, Q_t^e)$ . For an action  $a_t = (q_t^r, q_t^e)$ , the corresponding total cost at time  $t$  is

$$c_t(s_t, a_t) = c_r q_t^r + c_e q_t^e + h[I_t + q_{t-l_r}^r + q_{t-l_e}^e - D_t]^+ + b[D_t - I_t - q_{t-l_r}^r - q_{t-l_e}^e]^+, \quad (15)$$

where  $[x]^+ = \max(0, x)$ , and  $h$  and  $b$  are the holding and shortage costs, respectively. We use  $\mathcal{S}_t$  and  $\mathcal{A}_t(s_t)$  to denote the sets of all admissible states and order policies at time  $t$ , respectively.

It is well-known that Eq. (3) admits a stationary optimal policy  $\pi^*$  for dual sourcing when the demand distribution has a finite support over the time horizon  $T$  (Hua et al. 2015). The general optimal policy for dual sourcing problems has not been characterized analytically. We describe the numerical procedure that we use to compute optimal order policies for small-scale dual sourcing instances in the electronic companion that accompanies this paper.

## 5.2. Approximating Optimal Dual-Sourcing Policies

Our goal is to design IDINNs that are able to solve dual-sourcing inventory management problems that have no known analytical solution. Similar to the neural-network architecture used in the single-sourcing problem, we employ a neural network that uses as an input the  $(l_r + l_e + 1)$ -dimensional state  $s_t = (I_{t-1}, Q_{t-1}^r, Q_{t-1}^e)$  [Figure 3(a)]. After processing the inputs in a set of hidden layers, the neural network outputs the action  $\hat{a}_t = (\hat{q}_t^r, \hat{q}_t^e)$ . Note that actions that are generated by a neural network depend on its weights, that is,  $\hat{a}_t = \hat{a}_t(\mathbf{w})$ . For training the neural network, we calculate the expected total cost over  $T$  periods (15). Neural network weights and biases, indicated by “+1s” in Figure 3(a), are adjusted by backpropagating gradients that result from expected-cost minimization. As in the previous section, we backpropagate gradients using fractional decoupling [see Eq. (11)]. The main steps of the training algorithm are summarized in Algorithm 1. In lines 6-13 the algorithm evaluates an ordering policy implied by the neural network weights  $\mathbf{w}^{(n)}$ . The outer loop in lines 4-13 performs the order optimization using gradient descent on the neural network weights  $\mathbf{w}$ . All neural networks that we use in our numerical experiments consist of seven fully connected, hidden layers with 128, 64, 32, 16, 8, 4, and 2 CELU neurons, respectively. For more details on the network structure and learning dynamics, we refer the reader to the e-companion.

---

**Algorithm 1** A generic algorithm that describes a simplified training procedure of IDINNs for controlling dual-sourcing problems. An IDINN represents the order policy  $\hat{\pi}$  that depends on the neural-network parameters  $\mathbf{w}$ .

---

```

1: Inputs:
    $\phi, c_r, c_e, l_r, l_e, h, b, T, M, \eta, \text{NN\_CONTROLLER}(), \text{INVENTORY\_DYNAMICS}()$ 
2: Outputs:
   best_loss,  $\mathbf{w}^*$ 
3: Initialize:
    $\mathbf{w}^{(1)}, \mathbf{s}_1^{(1)}, \dots, \mathbf{s}_1^{(M)}$ 
4: for n = 1 to max_epochs do ▷ Iterate over all training epochs.
5:   total_cost  $\leftarrow 0$ 
6:   for t = 1 to T do ▷ Iterate over discrete time steps in a time horizon [1, T].
7:     mean_cost  $\leftarrow 0$ 
8:     for m = 1 to M do ▷ Iterate over all samples in a mini-batch.
9:        $D_t^{(m)} \sim \phi$  ▷ Sample from a demand distribution, e.g., a uniform distribution.
10:       $\hat{q}_t^r, \hat{q}_t^e \leftarrow \text{NN\_CONTROLLER}(\mathbf{s}_t^{(m)}, \mathbf{w}^{(n)})$  ▷ NN controller calculates current orders.
11:       $\mathbf{s}_{t+1}^{(m)}, c_t^{(m)} \leftarrow \text{INVENTORY\_DYNAMICS}(D_t^{(m)}, \mathbf{s}_t^{(m)}, \hat{q}_t^r, \hat{q}_t^e)$  ▷ State update (14, 15).
12:      mean_cost  $+= c_t^{(m)} / M$  ▷ Calculate mean cost over all samples per time step.
13:     end for
14:     total_cost  $+= \text{mean\_cost}$ 
15:   end for
16:    $J^{(\hat{\pi}_t)} \leftarrow \text{total\_cost}$  ▷ Set the learning loss as the expected total cost over all samples.
17:    $\mathbf{w}^{(n+1)} \leftarrow \mathbf{w}^{(n)} - \eta \nabla_{\mathbf{w}^{(n)}} J^{(\hat{\pi}_t)}$  ▷ Perform a gradient descent step for NN parameters.
   ▷ Other parameter update methods (e.g., RMSProp) can be used in this step as well.
18:   if total_cost < best_loss then ▷ Check for best performance over epochs 1, ..., n.
19:      $\mathbf{w}^* \leftarrow \mathbf{w}^{(n+1)}$  ▷ Save best neural-network parameters  $\mathbf{w}^*$ .
20:     best_loss  $\leftarrow \text{total\_cost}$ 
21:   end if
22: end for
23: return best_loss,  $\mathbf{w}^*$ 

```

---

## 6. Computational Experiments

We carry out computational experiments to shed light on a matter of aspects pertinent to our method's performance, which we organize in three parts. The first part demonstrates performance in terms of the expected cost per period, when compared to the optimal solution and to an alternative,

state-of-the-art benchmark. In addition, we illustrate to what extent IDINNs approximate optimal solutions not only in the sense of obtaining near-optimal cost values, but also in how these values are distributed in a variety of samples. The second part extends the analysis of the first part to a larger set of instances, and compares the neural network control approach with the optimal solutions and the alternative benchmark. We apply transfer learning to take advantage of existing ordering policies and warm-start the neural network training. Transfer learning can help to reduce the number of training epochs by a factor between 10 and 30, depending on the instance. Moreover, in this part we study the ability of IDINNs to approximate optimal solutions in a stronger sense, namely its ability to generate ordering policies that are close to the optimal ones. Finally, the third part applies neural network control on a subset of real demand data, obtained by Manary and Willems (2021), and shows how it can outperform an alternative approach.

In all our experiments, we compare the neural network’s performance with the capped dual index heuristic (CDI) that first appeared in Sun and Van Mieghem (2019). The CDI policy is an appropriate benchmark for several reasons. First, it can be seen as a generalized version of the tailor-based surge heuristic, which is asymptotically optimal for large  $l_r$  (Xin and Goldberg 2018). Second, it is easy to understand, implement and communicate, and as such it is an appropriate baseline for a more complex approach. Finally, it has state-of-the-art performance, which, combined with its simplicity (only 3 parameters need to be optimized), make it favorable against more complex approaches that may outperform it marginally.

Experiments were carried out on an AMD<sup>®</sup> Ryzen threadripper 3970. In this machine, 100 training epochs take about 20 seconds to complete. Without having access to a pretrained neural network, obtaining optimality gaps of about 0.1% requires between 2,000 and 3,000 training epochs, which corresponds to less than 10 minutes of CPU time. Pretrained neural networks can achieve good performance on unseen instances after training them for a few hundred epochs. For comparison, dynamic programming solutions of certain instances took about 50 days of computing time. All implementations are available on Gitlab, while some details of the corresponding algorithms are also summarized in the e-companion.

### 6.1. Visualizing IDINN performance

In this part, we use nine small instances with discrete uniform demand distribution  $\mathcal{U}\{0,4\}$ , and parameters  $h = 5, b = 495, c_e \in \{5, 10, 20\}$  and  $l_r \in \{2, 3, 4\}$ . In all experiments, we set  $c_r = 0$  and  $l_e = 0$  without loss of generality (Sheopuri et al. 2010). The latter assumption is justified because any system with  $l_e > 0$  can be transformed to an equivalent one with  $l_e = 0$  (Sun and Van Mieghem 2019, Xin 2021a). Such small instances have been used in the literature to evaluate various heuristics (Scheller-Wolf et al. 2007, Gijsbrechts et al. 2020). Their advantage is that exact optimal solutions

can be obtained, and therefore one can evaluate performance in a formal sense. We use these instances to investigate the performance and structure of solutions obtained by our approach. A potential limitation of such instances is that it is not clear whether a method that performs well in such small instances will perform well in more realistic demand distributions. We address this point using real demand data in the third part of our analysis.

Panel (a) of Figure 3 shows the generic design of the network, while panel (b) shows the evolution of the expected cost per period during learning for  $l_r = 2$ ,  $c_e = 20$ , and  $T = 100$ . We observe that the cost reaches values below 100 after a few training epochs and approaches the optimal solution after about 2,500 epochs (*i.e.*, after a few minutes of CPU time). Panels (c–k) show the cumulative distribution functions (CDFs) of the expected costs per period for  $c_e = 20, 10, 5$  (from left to right) and  $l_r = 2, 3, 4$  (from top to bottom). Distributions are formed by 500 realizations, each consisting of a time horizon  $T = 1,000$ . The dashed black line indicates the corresponding infinite horizon optimal expected cost per period (numerical values are reported in Table 1). We observe that IDINN-based order policies stochastically dominate CDI in seven of out nine instances. For the remaining two instances, IDINN-based policies have an average cost that matches that of CDI. In conclusion, these experiments imply that IDINN has comparable – and even better – performance to CDI. The absolute cost difference is small, because both methods are near optimal. However, what is perhaps unexpected is the consistency by which IDINN outperforms CDI, not only in terms of average cost, but also on a realization-by-realization basis, as illustrated by panels (c–k).

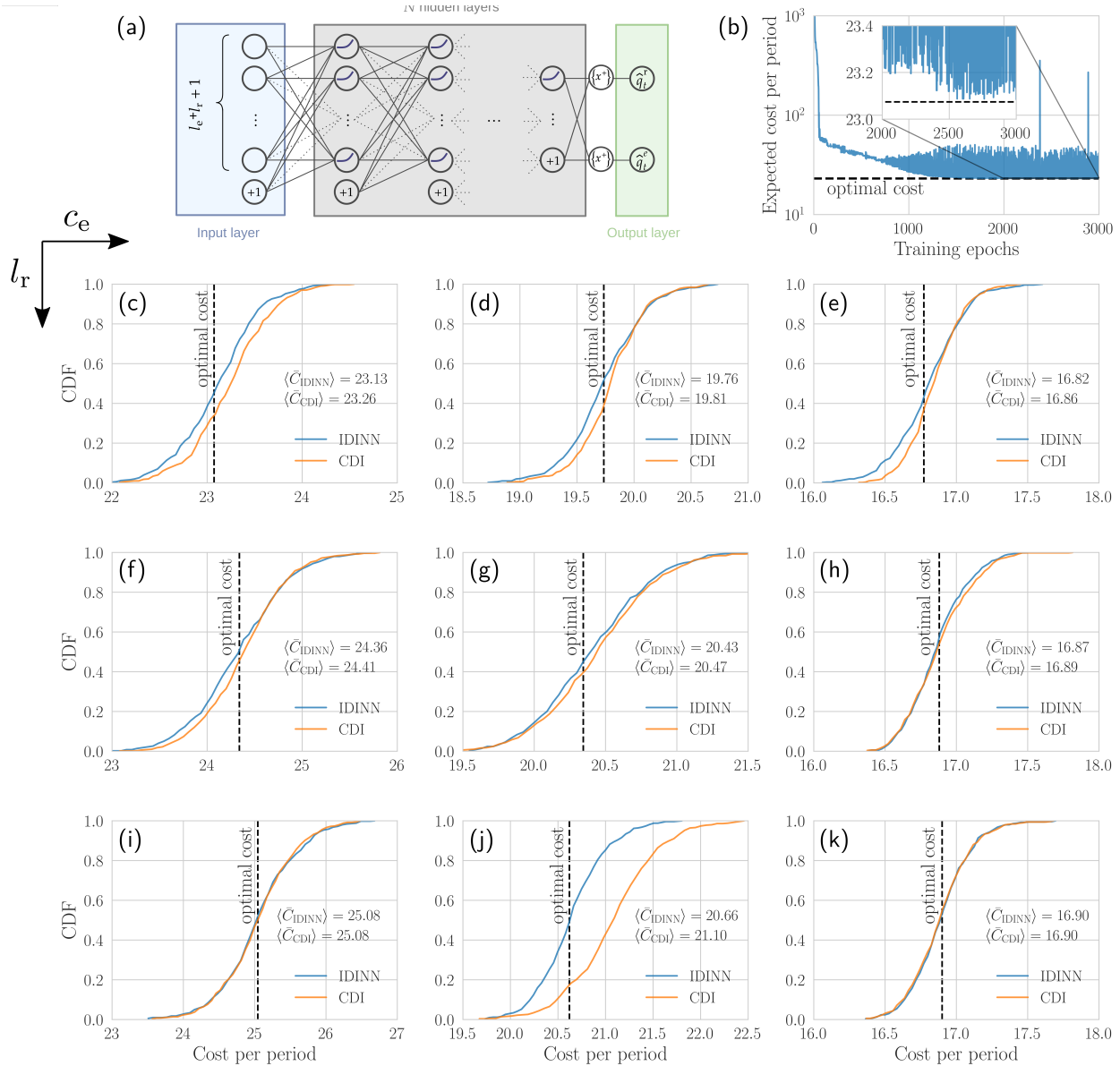
## 6.2. Learning Optimal Solutions

We now extend the set of instances to include two backlog cost levels ( $b \in \{95, 495\}$ ) and two demand distributions ( $\mathcal{U}\{0, 4\}$  and  $\mathcal{U}\{0, 8\}$ ). The IDINN, CDI, and DP expected costs per period of these instances are summarized in Table 1. In all 36 instances, the cost of IDINN-based order policies is lower or equal than that of corresponding optimized CDI policies. For the majority of neural networks that we used to generate the results shown in Tab. 1, we employed a transfer-learning approach (Bozinovski and Fulgosi 1976) to speed-up training. We found that with transfer learning some neural networks reached a good performance after a few hundred training epochs instead of after a few thousand training epochs, which corresponds to training times of less than 1 minute.

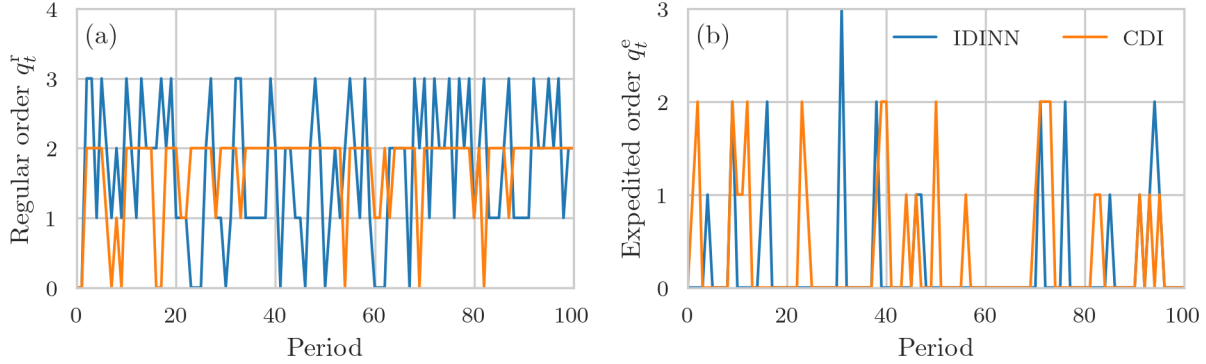
In order to quantify the similarity of optimal solution, we measure the root mean square (RMSE) distance of CDI and IDINN against the known optimal solutions. Specifically, if  $\mathcal{S}_{\text{DP}}$  is the set of recurrent states in the obtained optimal solution, we define RMSE of method  $m$  as

$$\text{RMSE}_m = \sqrt{\frac{1}{|\mathcal{S}_{\text{DP}}|} \sum_{s \in \mathcal{S}_{\text{DP}}} (q_{\text{DP}}^r(s) - q_m^r(s))^2 + (q_{\text{DP}}^e(s) - q_m^e(s))^2}, \quad (16)$$

**Figure 3** Training of neural network control and average cost distribution for dual-sourcing inventory management.



*Note.* (a) Schematic of IDINN architecture for dual sourcing. The neural network uses as an input the  $(l_r + l_e + 1)$ -dimensional state  $s_t = (I_{t-1}, Q_{t-1}^r, Q_{t-1}^e)$  and outputs an action  $\hat{a}_t = (\hat{q}_t^r, \hat{q}_t^e)$ . Hidden layers are composed of CELU activations and bias terms, indicated by “+1”s. (b) Expected cost per period as a function of training epochs for  $h = 5$ ,  $b = 495$ ,  $c_r = 0$ ,  $c_e = 20$ ,  $l_r = 2$ ,  $l_e = 0$ ,  $T = 100$ , and demand distribution  $\mathcal{U}\{0, 4\}$ . The dashed black line indicates the approximately optimal cost value found with a dynamic programming approach. (c–k) Cumulative distribution functions (CDFs) of the cost per period for CDI and IDINN policies. The shown distributions are based on 500 realizations, each consisting of a time horizon  $T = 1,000$ . Expedited order costs are 20, 10, and 5 (from left to right); regular order lead time are 2, 3, and 4 (from top to bottom). The expected costs per period associated with IDINN and CDI policies are denoted  $\langle \bar{C}_{IDINN} \rangle$  and  $\langle \bar{C}_{CDI} \rangle$ , respectively. Order policies that are based on IDINNs stochastically dominate CDI in seven out of nine instances. In the remaining two cases, the performance is almost identical.

**Figure 4** Comparison of IDINN and CDI orders.

*Note.* Evolution of IDINN and CDI regular orders (a) and expedited orders (b). The parameters of the underlying dual sourcing problem are  $h = 5$ ,  $b = 495$ ,  $c_r = 0$ ,  $c_e = 20$ ,  $l_r = 2$ , and  $l_e = 0$ . The demand distribution is  $\mathcal{U}\{0, 4\}$ .

where  $q_{\text{DP}}^r(s)$  and  $q_{\text{DP}}^e(s)$  respectively denote the optimal (“dynamic program”) regular and expedited orders associated with state  $s$ . The corresponding regular and expedited orders of method  $m$  are  $q_m^r(s)$  and  $q_m^e(s)$ , respectively. In our experiments,  $\mathcal{S}_{\text{DP}}$  is a subset of the recurrent states of both CDI and IDINN. To this end, the last two columns of Table 1 show the corresponding RMSEs. We see that IDINNs have a lower average and median RMSE compared to CDI (0.51 vs 0.59; 0.50 vs 0.57, respectively); IDINNs attain a lower RMSE in more than half the instances. It should be noted that IDINNs are trained in the original state space, while the states of the DP and CDI are in the compact,  $l_r$ -dimensional space. When we convert the IDINN ordering policies in the compact space, we average the corresponding ordering quantities. The resulting fractional ordering quantities can be interpreted as randomized ordering policies.

Figure 4 shows an example of the evolution of regular and expedited orders that are based on IDINN and CDI policies. We observe that CDI regular orders are bounded from above by 4, limiting the ability of CDI to respond to demand fluctuations that require larger regular orders. One advantage of IDINN-based policies over CDI is that regular orders can be placed in a way that is tailored to the current inventory and previously placed orders. As a result, fewer expedited orders need to be placed to replenish inventory.

**Table 1** Expected costs per period of CDI and IDINN-based order policies.

$l_r$	$c_e$	$b$	demand	CDI cost	IDINN cost	DP cost	CDI RMSE	IDINN RMSE
2	5	95	$\mathcal{U}\{0, 4\}$	16.87	<b>16.80</b>	16.77	0.58	<b>0.56</b>
2	5	95	$\mathcal{U}\{0, 8\}$	32.41	<b>32.33</b>	32.27	<b>0.31</b>	0.57
2	5	495	$\mathcal{U}\{0, 4\}$	16.86	<b>16.82</b>	16.77	0.58	<b>0.48</b>
2	5	495	$\mathcal{U}\{0, 8\}$	<b>32.28</b>	<b>32.28</b>	32.27	<b>0.31</b>	0.50
2	10	95	$\mathcal{U}\{0, 4\}$	19.81	<b>19.79</b>	19.73	<b>0.40</b>	0.56
2	10	95	$\mathcal{U}\{0, 8\}$	37.42	<b>37.24</b>	37.24	0.57	<b>0.45</b>
2	10	495	$\mathcal{U}\{0, 4\}$	19.81	<b>19.76</b>	19.74	0.40	<b>0.26</b>
2	10	495	$\mathcal{U}\{0, 8\}$	<b>37.92</b>	<b>37.92</b>	37.84	0.60	<b>0.52</b>
2	20	95	$\mathcal{U}\{0, 4\}$	23.01	<b>22.99</b>	22.83	0.54	<b>0.50</b>
2	20	95	$\mathcal{U}\{0, 8\}$	41.73	<b>41.68</b>	41.64	0.65	<b>0.46</b>
2	20	495	$\mathcal{U}\{0, 4\}$	23.26	<b>23.13</b>	23.07	0.46	<b>0.45</b>
2	20	495	$\mathcal{U}\{0, 8\}$	43.82	<b>43.79</b>	43.77	0.54	<b>0.40</b>
3	5	95	$\mathcal{U}\{0, 4\}$	<b>16.88</b>	<b>16.88</b>	16.88	0.53	<b>0.43</b>
3	5	95	$\mathcal{U}\{0, 8\}$	32.93	<b>32.65</b>	32.60	0.86	<b>0.49</b>
3	5	495	$\mathcal{U}\{0, 4\}$	16.89	<b>16.87</b>	16.88	0.53	<b>0.44</b>
3	5	495	$\mathcal{U}\{0, 8\}$	32.80	<b>32.66</b>	32.60	<b>0.86</b>	0.93
3	10	95	$\mathcal{U}\{0, 4\}$	20.48	<b>20.40</b>	20.34	<b>0.36</b>	0.37
3	10	95	$\mathcal{U}\{0, 8\}$	38.79	<b>38.69</b>	38.64	0.64	<b>0.58</b>
3	10	495	$\mathcal{U}\{0, 4\}$	20.47	<b>20.43</b>	20.34	<b>0.36</b>	0.77
3	10	495	$\mathcal{U}\{0, 8\}$	39.10	<b>38.97</b>	38.89	0.97	<b>0.77</b>
3	20	95	$\mathcal{U}\{0, 4\}$	24.44	<b>24.43</b>	24.30	0.57	<b>0.49</b>
3	20	95	$\mathcal{U}\{0, 8\}$	44.70	<b>44.59</b>	44.44	<b>0.61</b>	<b>0.61</b>
3	20	495	$\mathcal{U}\{0, 4\}$	24.41	<b>24.36</b>	24.34	0.44	<b>0.33</b>
3	20	495	$\mathcal{U}\{0, 8\}$	46.39	<b>46.33</b>	46.20	<b>0.57</b>	0.63
4	5	95	$\mathcal{U}\{0, 4\}$	<b>16.90</b>	<b>16.90</b>	16.90	0.57	<b>0.51</b>
4	5	95	$\mathcal{U}\{0, 8\}$	32.95	<b>32.82</b>	32.71	0.80	<b>0.62</b>
4	5	495	$\mathcal{U}\{0, 4\}$	<b>16.90</b>	<b>16.90</b>	16.90	0.57	<b>0.50</b>
4	5	495	$\mathcal{U}\{0, 8\}$	32.94	<b>32.72</b>	32.72	0.80	<b>0.58</b>
4	10	95	$\mathcal{U}\{0, 4\}$	21.10	<b>20.69</b>	20.61	0.55	<b>0.44</b>
4	10	95	$\mathcal{U}\{0, 8\}$	39.63	<b>39.49</b>	39.25	1.10	<b>0.60</b>
4	10	495	$\mathcal{U}\{0, 4\}$	21.10	<b>20.66</b>	20.61	0.55	<b>0.38</b>
4	10	495	$\mathcal{U}\{0, 8\}$	39.63	<b>39.45</b>	39.35	0.86	<b>0.45</b>
4	20	95	$\mathcal{U}\{0, 4\}$	<b>25.08</b>	<b>25.08</b>	24.56	<b>0.36</b>	0.51
4	20	95	$\mathcal{U}\{0, 8\}$	46.46	<b>46.14</b>	46.02	0.84	<b>0.44</b>
4	20	495	$\mathcal{U}\{0, 4\}$	<b>25.08</b>	<b>25.08</b>	25.04	<b>0.32</b>	0.37
4	20	495	$\mathcal{U}\{0, 8\}$	47.66	<b>47.56</b>	47.53	0.63	<b>0.39</b>

CDI and IDINN costs are based on 500 realizations, each consisting of a time horizon  $T = 1,000$ . For comparison, we also show the corresponding infinite-horizon DP cost. The parameters  $l_r$ ,  $c_e$ , and  $b$  and the demand distribution are as listed in the first four columns. The remaining parameters are held constant at  $c_r = 0$  and  $h = 5$ .

### 6.3. Controlling Real-World Inventory Management Problems

We now apply IDINNs to dual-sourcing problems with actual customer demand data taken from Manary and Willems (2021). The data represent customer demand of microprocessors from Intel Corporation. Contrary to the previous datasets, that assumed stationary demand, this dataset models a situation where demand evolves to a peak, then plateaus, and eventually vanishes. Such a demand profile corresponds to the introduction of a new microprocessor generation: at the initial stage, it replaces older microprocessors, then it enjoys a maturity period, and eventually it is replaced by a new generation. Figure 5(a) shows the evolution of customer demand over  $T = 120$  weeks. Each grey line represents different microprocessor generations, and is used to generate sample paths for future demand. We describe such empirical demand data by a Gaussian process (Roberts et al. 2013) with random demand

$$D_t \sim \mathcal{N}^+(\mu_t, \sigma_t, a, b) \quad t \in \{1, \dots, T\}, \quad (17)$$

where  $\mathcal{N}^+(\mu_t, \sigma_t, a, b)$  denotes a truncated normal distribution with domain  $(a, b)$ . The quantities  $\mu_t$  and  $\sigma_t$  denote mean and standard deviation of the empirical demand data at time  $t$ . The solid red line in Figure 5(a) shows the evolution of the mean  $\mu_t$  and grey-shaded regions indicate the 95% confidence intervals (CIs). Demands are zero in the beginning of the shown product lifecycle. The peak demand reaches values of about  $3 \times 10^5$  units after about 70 weeks. To reduce the effect of truncation errors, we chose a relatively broad truncation interval  $(a, b) = (0, 10^8)$ . The key difference between this environment and the archetypal dual sourcing problem is the finite time horizon. Note that CDI remains robustly optimal for finite time horizons with non-stationary, correlated demand confined to polyhedral uncertainty sets. Therefore, it remains a competitive benchmark, to which we compare IDINNs' performance.

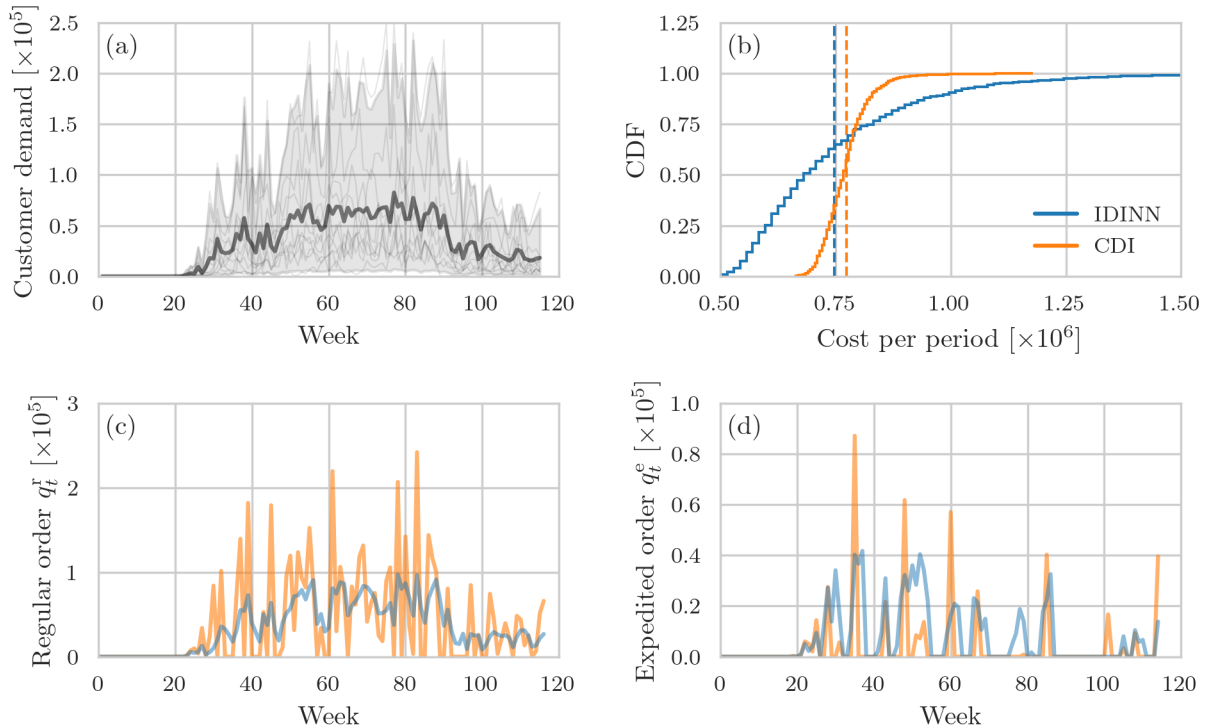
To calculate CDI orders, we determine the order-up-to levels of the regular and expedited suppliers,  $S_t^{r*}$  and  $S_t^{e*}$ , and the cap  $\bar{q}_t^{r*}$  (see the e-companion for further details) by estimating the minimum and maximum demand using estimates of the 99% CIs of the distribution  $\mathcal{N}^+(\mu_t, \sigma_t, a, b)$ . That is,

$$\begin{aligned} S_t^{e*} &= \bar{q}_t^{r*} = \frac{h[\mu_t - 2.58\sigma_t]^+ + b[\mu_t + 2.58\sigma_t]}{h + b}, \\ S_t^{r*} &= \frac{hl[\mu_t - 2.58\sigma_t]^+ + bl[\mu_t + 2.58\sigma_t]}{h + b}, \end{aligned} \quad (18)$$

where  $l = l_r - l_e$ .

For a meaningful comparison between IDINNs and CDI, we let the neural network access  $\mu_t$  and  $\sigma_t$ . Specifically, the neural network input consists of (i)  $Q_t^r, Q_t^e$ , the order pipelines associated with slow and fast orders, respectively; and (iii)  $\mu_t, \sigma_t$ , the mean and standard deviation of the

**Figure 5** Controlling real-world inventory management problems with IDINNs and CDI.



*Note.* (a) Customer demand data (solid grey lines) that is taken from Manary and Willems (2021). The solid black line and grey-shaded regions indicate the mean customer demand and 95% confidence intervals of the demand distribution (17), respectively. (b) The cumulative distribution function of the average IDINN and CDI costs. Shown results are based on  $10^3$  i.i.d. samples. Dashed lines indicate mean expected costs per period [747,117 (IDINN) and 773,993 (CDI)]. (c) An example of regular orders generated by an IDINN (solid blue line) and a CDI policy (solid orange line). (d) An example of expedited orders generated by an IDINN (solid blue line) and a CDI policy (solid orange line). The parameters of the underlying dual sourcing problem are  $h = 5$ ,  $b = 495$ ,  $c_r = 0$ ,  $c_e = 20$ ,  $l_r = 2$ , and  $l_e = 0$ .

time-varying demand. Preliminary experiments with different input representations, such as the  $l$ -component representation of state, did not show any material difference in the results. More details on the employed neural-network structure and training algorithm (“one-shot learning”) are reported in the e-companion.

To compare the performance of IDINN and CDI-based policies for real-world inventory management problems, we generate 1,000 i.i.d. samples for  $h = 5$ ,  $b = 495$ ,  $c_r = 0$ ,  $c_e = 20$ ,  $l_r = 2$ , and  $l_e = 0$ . We find that IDINNs outperform CDI in more than 65% of the studied realizations. The median expected costs per period are 692,118 (IDINN) and 770,362 (CDI); the mean expected costs per period are 747,117 (IDINN) and 773,993 (CDI) [dashed lines in Figure 5(b)]. We also evaluate the differences between CDI and IDINN costs using the Wilcoxon signed-rank test (Wilcoxon 1992). Our analysis shows that the null hypothesis that the difference between the CDI and IDINN median costs is negative can be rejected ( $p < 10^{-10}$ ) in favor of the alternative that the median

cost difference is greater than zero. For a further comparison between IDINNs and CDI, we set the backlog cost  $b = 95$  and again analyze the expected costs per period using 1,000 i.i.d. samples. We find that the advantage of IDINNs over CDI is even more pronounced in this example with a smaller backlog cost. The median expected costs per period are 563,711 (IDINN) and 735,265 (CDI) and the mean expected costs per period are 583,873 (IDINN) and 736,018 (CDI). In relative terms, the reduction on average cost is 20%, which constitutes a significant improvement over the CDI policy.

Figure 5(c,d) shows an example of regular and expedited orders that are generated by an IDINN policy (solid blue lines) and a CDI policy (solid orange lines). We observe that the IDINN regular orders fluctuate to a lesser degree between very high and very low orders than those of the employed CDI order policy. Another difference between the shown IDINN and CDI policies is that CDI tends to replenish inventory with larger expedited orders.

To summarize, we have shown that IDINNs are able to learn effective order policies that solve inventory management problems with empirical demand data. In the above examples, IDINN-based order policies can lead to savings between 3–20% compared to an effective state-of-the-art heuristic.

## 7. Conclusion

Our work develops a neural-network-based inventory management system that directly learns effective order policies by minimizing the backlogging, holding, and sourcing costs of underlying inventory dynamics.

We have shown that one activation function suffices for inventory-dynamics neural networks (IDINNs) to learn the optimal order policy of single-sourcing problems. Extending the structure of the single-sourcing neural network, we developed IDINNs that are able to outperform state-of-the-art order heuristics in dual-sourcing problems. Finally, we demonstrated the ability of IDINNs to control inventory management problems with empirical demand data. In all studied instances, IDINNs either outperformed state-of-the-art baselines or achieved equal performance. Training times varied between a few minutes to about one hour on a regular personal computer. All trained neural networks are publicly available (see e-companion) and may be used as a starting point for solving related inventory management problems via transfer learning.

Future research may explore the application of inventory-dynamics-informed neural networks to partially observable inventory management problems, different demand distributions, and complex, multi-constraint optimization problems such as effective vaccine distribution (Mak et al. 2021). Another promising venue for research is the application of neural-network-based inventory management systems to continuous-time models (Xin and Van Mieghem 2021).

## References

- Allon G, Van Mieghem JA (2010) Global dual sourcing: Tailored base-surge allocation to near-and offshore production. *Management Science* 56(1):110–124.
- Arrow KJ, Harris T, Marschak J (1951) Optimal inventory policy. *Econometrica: Journal of the Econometric Society* 250–272.
- Asikis T (2021) Multi-objective optimization for value-sensitive and sustainable basket recommendations. *arXiv preprint arXiv:2111.05944* .
- Asikis T, Böttcher L, Antulov-Fantulin N (2020) Neural Ordinary Differential Equation Control of Dynamics on Graphs. *Physical Review Research* (in press) .
- Barankin E (1963) A delivery-lag inventory model with an emergency provision. Technical report, CALIFORNIA UNIV BERKELEY STATISTICAL LAB.
- Barron JT (2017) Continuously differentiable exponential linear units. *arXiv preprint arXiv:1704.07483* .
- Baydin AG, Pearlmutter BA, Radul AA, Siskind JM (2018) Automatic differentiation in machine learning: a survey. *Journal of machine learning research* 18.
- Bellman R (1954) The theory of dynamic programming. Technical report, Rand Corporation.
- Bertsekas DP (2011) Dynamic Programming and Optimal Control: Volume II (3rd edition). *Belmont, MA: Athena Scientific* II.
- Böttcher L, Antulov-Fantulin N, Asikis T (2022) AI Pontryagin or how neural networks learn to control dynamical systems. *Nature Communications* .
- Boute RN, Disney SM, Gijsbrechts J, Van Mieghem JA (2021a) Dual sourcing and smoothing under non-stationary demand time series: Reshoring with speed factories. *Management Science* .
- Boute RN, Gijsbrechts J, van Jaarsveld W, Vanvuchelen N (2021b) Deep reinforcement learning for inventory control: a roadmap. *European Journal of Operational Research* .
- Bozinovski S, Fulgosi A (1976) The influence of pattern similarity and transfer learning upon the training of a base perceptron B2.(original in croatian). *Proceedings of the Symposium Informatica*, 3–121.
- Chen B, Shi C (2019) Tailored base-surge policies in dual-sourcing inventory systems with demand learning. *Available at SSRN 3456834* .
- Chen RT, Amos B, Nickel M (2020) Learning Neural Event Functions for Ordinary Differential Equations. *arXiv preprint arXiv:2011.03902* .
- Clevert DA, Unterthiner T, Hochreiter S (2015) Fast and accurate deep network learning by exponential linear units (elus). *arXiv preprint arXiv:1511.07289* .
- DeCroix GA, Arreola-Risa A (1998) Optimal production and inventory policy for multiple products under resource constraints. *Management Science* 44(7):950–961.

- Douglas SC, Yu J (2018) Why ReLU units sometimes die: analysis of single-unit error backpropagation in neural networks. *2018 52nd Asilomar Conference on Signals, Systems, and Computers*, 864–868 (IEEE).
- Fei-Fei L, Fergus R, Perona P (2006) One-shot learning of object categories. *IEEE Transactions on Pattern Analysis and Machine Intelligence* 28(4):594–611.
- Fukuda Y (1964) Optimal policies for the inventory problem with negotiable leadtime. *Management Science* 10(4):690–708.
- Gijsbrechts J, Boute RN, Van Mieghem JA, Zhang D (2020) Can deep reinforcement learning improve inventory management? Performance on dual sourcing, lost sales and multi-echelon problems. *Performance on Dual Sourcing, Lost Sales and Multi-Echelon Problems (October 6, 2020)* .
- Goldberg DA, Reiman MI, Wang Q (2021) A survey of recent progress in the asymptotic analysis of inventory systems. *Production and Operations Management* 30(6):1718–1750.
- Hanin B, Sellke M (2017) Approximating continuous functions by ReLU nets of minimal width. *arXiv preprint arXiv:1710.11278* .
- Hinton G (2016) RMSprop — PyTorch 1.10.0 documentation. URL <https://pytorch.org/docs/stable/generated/torch.optim.RMSprop.html>.
- Holl P, Thuerey N, Koltun V (2020) Learning to Control PDEs with Differentiable Physics. *8th International Conference on Learning Representations, ICLR 2020, Addis Ababa, Ethiopia, April 26-30, 2020* (OpenReview.net), URL <https://openreview.net/forum?id=HyeSin4FPB>.
- Hornik K (1991) Approximation capabilities of multilayer feedforward networks. *Neural Networks* 4(2):251–257.
- Hua Z, Yu Y, Zhang W, Xu X (2015) Structural properties of the optimal policy for dual-sourcing systems with general lead times. *IIE Transactions* 47(8):841–850.
- Janakiraman G, Seshadri S, Sheopuri A (2015) Analysis of tailored base-surge policies in dual sourcing inventory systems. *Management Science* 61(7):1547–1561.
- Jin C, Allen-Zhu Z, Bubeck S, Jordan MI (2018) Is q-learning provably efficient? *arXiv preprint arXiv:1807.03765* .
- Jin W, Wang Z, Yang Z, Mou S (2020) Pontryagin Differentiable Programming: An End-to-End Learning and Control Framework. Larochelle H, Ranzato M, Hadsell R, Balcan M, Lin H, eds., *Advances in Neural Information Processing Systems 33: Annual Conference on Neural Information Processing Systems 2020, NeurIPS 2020, December 6-12, 2020, virtual*, URL <https://proceedings.neurips.cc/paper/2020/hash/5a7b238ba0f6502e5d6be14424b20ded-Abstract.html>.
- Karniadakis GE, Kevrekidis IG, Lu L, Perdikaris P, Wang S, Yang L (2021) Physics-informed machine learning. *Nature Reviews Physics* 3(6):422–440.

- Kingma DP, Ba J (2014) Adam: A method for stochastic optimization. *arXiv preprint arXiv:1412.6980* .
- Li M, Zhang T, Chen Y, Smola AJ (2014) Efficient mini-batch training for stochastic optimization. *Proceedings of the 20th ACM SIGKDD international conference on Knowledge discovery and data mining*, 661–670.
- Linnainmaa S (1976) Taylor expansion of the accumulated rounding error. *BIT Numerical Mathematics* 16(2):146–160.
- Lutter M, Ritter C, Peters J (2019) Deep Lagrangian Networks: Using Physics as Model Prior for Deep learning. *7th International Conference on Learning Representations, ICLR 2019, New Orleans, LA, USA, May 6-9, 2019* (OpenReview.net), URL <https://openreview.net/forum?id=BklHpjCqKm>.
- Mak HY, Dai T, Tang CS (2021) Managing two-dose COVID-19 vaccine rollouts with limited supply. *Available at SSRN 3790836* .
- Manary MP, Willems SP (2021) Data Set: 187 Weeks of Customer Forecasts and Orders for Microprocessors from Intel Corporation. *Manufacturing & Service Operations Management* .
- Masters D, Luschi C (2018) Revisiting small batch training for deep neural networks. *arXiv preprint arXiv:1804.07612* .
- Morton TE (1971) The near-myopic nature of the lagged-proportional-cost inventory problem with lost sales. *Operations Research* 19(7):1708–1716.
- Nair V, Hinton GE (2010) Rectified Linear Units Improve Restricted Boltzmann Machines. Fürnkranz J, Joachims T, eds., *Proceedings of the 27th International Conference on Machine Learning (ICML-10), June 21-24, 2010, Haifa, Israel*, 807–814 (Omnipress), URL <https://icml.cc/Conferences/2010/papers/432.pdf>.
- Park S, Yun C, Lee J, Shin J (2020) Minimum width for universal approximation. *arXiv preprint arXiv:2006.08859* .
- Paszke A, Gross S, Chintala S, Chanan G, Yang E, DeVito Z, Lin Z, Desmaison A, Antiga L, Lerer A (2017) Automatic differentiation in PyTorch .
- Polydoros AS, Nalpantidis L (2017) Survey of model-based reinforcement learning: Applications on robotics. *Journal of Intelligent & Robotic Systems* 86(2):153–173.
- Powell WB (2007) *Approximate Dynamic Programming: Solving the curses of dimensionality*, volume 703 (John Wiley & Sons).
- Raissi M, Perdikaris P, Karniadakis GE (2019) Physics-informed neural networks: A deep learning framework for solving forward and inverse problems involving nonlinear partial differential equations. *Journal of Computational Physics* 378:686–707.
- Roberts S, Osborne M, Ebden M, Reece S, Gibson N, Aigrain S (2013) Gaussian processes for time-series modelling. *Philosophical Transactions of the Royal Society A: Mathematical, Physical and Engineering Sciences* 371(1984):20110550.

- Roehrl MA, Runkler TA, Brandtstetter V, Tokic M, Obermayer S (2020) Modeling system dynamics with physics-informed neural networks based on lagrangian mechanics. *IFAC-PapersOnLine* 53(2):9195–9200.
- Rumelhart DE, Hinton GE, Williams RJ (1986) Learning representations by back-propagating errors. *nature* 323(6088):533–536.
- Scarf H, Karlin S (1958) Inventory models of the arrow-harris-marschak type with time lag.
- Scheller-Wolf A, Veeraraghavan S, van Houtum GJ (2007) Effective dual sourcing with a single index policy. *Working Paper, Tepper School of Business, Carnegie Mellon University, Pittsburgh* .
- Schmidhuber J (2015) Deep learning in neural networks: An overview. *Neural Networks* 61:85–117.
- Sheopuri A, Janakiraman G, Seshadri S (2010) New policies for the stochastic inventory control problem with two supply sources. *Operations Research* 58(3):734–745.
- Song JS, van Houtum GJ, Van Mieghem JA (2020) Capacity and inventory management: Review, trends, and projections. *Manufacturing & Service Operations Management* 22(1):36–46.
- Song JS, Xiao L, Zhang H, Zipkin P (2017) Optimal policies for a dual-sourcing inventory problem with endogenous stochastic lead times. *Operations Research* 65(2):379–395.
- Song JS, Xiao L, Zhang H, Zipkin P (2021) Smart policies for multisource inventory systems and general tandem queues with order tracking and expediting. *Operations Research* .
- Song JS, Zipkin P (1993) Inventory control in a fluctuating demand environment. *Operations Research* 41(2):351–370.
- Sun J, Van Mieghem JA (2019) Robust dual sourcing inventory management: Optimality of capped dual index policies and smoothing. *Manufacturing & Service Operations Management* 21(4):912–931.
- Sutton RS, Barto AG (2018) *Reinforcement learning: An introduction* (MIT press).
- Van Hasselt H, Doron Y, Strub F, Hessel M, Sonnerat N, Modayil J (2018) Deep reinforcement learning and the deadly triad. *arXiv preprint arXiv:1812.02648* .
- Veeraraghavan S, Scheller-Wolf A (2008) Now or later: A simple policy for effective dual sourcing in capacitated systems. *Operations Research* 56(4):850–864.
- Veinott Jr AF (1965) The optimal inventory policy for batch ordering. *Operations Research* 13(3):424–432.
- Wang W, Axelrod S, Gómez-Bombarelli R (2020) Differentiable Molecular Simulations for Control and Learning. *CoRR* abs/2003.00868, URL <https://arxiv.org/abs/2003.00868>.
- Whittlemore AS, Saunders S (1977) Optimal inventory under stochastic demand with two supply options. *SIAM Journal on Applied Mathematics* 32(2):293–305.
- Wilcoxon F (1992) Individual comparisons by ranking methods. *Breakthroughs in statistics*, 196–202 (Springer).

- Xin L (2021a) 1.79-approximation algorithms for continuous review single-sourcing lost-sales and dual-sourcing inventory models. *Operations Research* .
- Xin L (2021b) Understanding the performance of capped base-stock policies in lost-sales inventory models. *Operations research* 69(1):61–70.
- Xin L, Goldberg DA (2018) Asymptotic optimality of tailored base-surge policies in dual-sourcing inventory systems. *Management Science* 64(1):437–452.
- Xin L, Van Mieghem JA (2021) Dual-sourcing, dual-mode dynamic stochastic inventory models: A review. *Dual-Mode Dynamic Stochastic Inventory Models: A Review (July 12, 2021)* .
- Yarats D, Zhang A, Kostrikov I, Amos B, Pineau J, Fergus R (2019) Improving sample efficiency in model-free reinforcement learning from images. *arXiv preprint arXiv:1910.01741* .
- Zhong YD, Dey B, Chakraborty A (2020) Symplectic ode-net: Learning hamiltonian dynamics with control. *8th International Conference on Learning Representations, ICLR 2020, Addis Ababa, Ethiopia, April 26-30, 2020* (OpenReview.net), URL <https://openreview.net/forum?id=ryxmb1rKDS>.
- Zipkin P (2008a) Old and new methods for lost-sales inventory systems. *Operations research* 56(5):1256–1263.
- Zipkin P (2008b) On the structure of lost-sales inventory models. *Operations research* 56(4):937–944.

## Sourcing Policies

In the following sections, we provide an overview of different dual sourcing heuristics that we use as baselines to evaluate the performance of inventory-dynamics-informed neural networks (IDINNs). Implementations of these sourcing policies and IDINNs are available at <https://gitlab.com/ComputationalScience/inventory-optimization>.

Although we focus on a comparison between IDINN and CDI policies in the main text, we will provide an overview of related single-index and dual-index policies for the sake of completeness. All of the aforementioned policies and TBS are also available at the GitLab repository and can be used for further comparisons.

### Single Index

In accordance with Scheller-Wolf et al. (2007), let  $z_e$  and  $z_r$  be the expedited and regular target order levels. The difference between  $z_r$  and  $z_e$  is denoted  $\Delta$ . For a single index policy, expedited and regular orders are chosen such that the inventory position at time  $t$  is  $\tilde{I}_t = z_r - D_{t-1} = z_e + \Delta - D_{t-1}$ . At the beginning of period  $t$ , an expedited order is placed according to

$$q_t^e = [z_e - \tilde{I}_t]^+ = [D_{t-1} - \Delta]^+. \quad (\text{EC.1})$$

The regular order in period  $t$  is

$$q_t^r = [z_r - (\tilde{I}_t + q_t^e)]^+ = [D_{t-1} - [D_{t-1} - \Delta]^+]^+ = D_{t-1} - q_t^e = \min(\Delta, D_{t-1}). \quad (\text{EC.2})$$

For the single index policy, the initial inventory level is  $I_0 = z_r$  and the inventory evolution satisfies ( $t > l_r$ )

$$\begin{aligned} I_{t+1} &= I_t + q_{t-l_r}^r + q_{t-l_e}^e - D_t = I_t + q_{t-l_e}^e - q_{t-l_r}^e - D_t + D_{t-l_r-1} \\ &= I_{t-1} + q_{t-l_e}^e - q_{t-l_r}^e + q_{t-l_e-1}^e - q_{t-l_r-1}^e - D_t - D_{t-1} + D_{t-l_r-1} + D_{t-l_r-2} \\ &= z_r + \sum_{i=0}^t (q_{t-l_e-i}^e - q_{t-l_r-i}^e) + \sum_{i=0}^t (D_{t-l_r-1-i} - D_i) \\ &= z_r + \sum_{i=t-l_r+1}^{t-l_e} q_i^e - \sum_{i=t-l_r}^t D_i \\ &= z_r + \sum_{i=t-l_r}^{t-l_e-1} [D_i - \Delta]^+ - \sum_{i=t-l_r}^{t-l_e-1} D_i - \sum_{i=t-l_e}^t D_i \\ &= z_r - \sum_{i=t-l_r}^{t-l_e-1} \min(\Delta, D_i) - \sum_{i=t-l_e}^t D_i \\ &= z_r - d_1(\Delta), \end{aligned} \quad (\text{EC.3})$$

where

$$d_1(\Delta) = \sum_{i=0}^{l_r - l_e - 1} \min(\Delta, D_i) + \sum_{i=0}^{l_e} D_i. \quad (\text{EC.4})$$

We use  $z_r^*$  to denote the value of the target order level leading to a minimum cost. To find the optimal  $z_r^*$ , observe that the ordering costs are independent of  $z_r$  since they are proportional to Eqs. (EC.1) and (EC.2). According to Eq. (EC.3), the optimal  $z_r^*$  can be determined by minimizing the expected holding and shortage costs

$$\begin{aligned} & h \int_0^{z_r} (z_r - x) f_{d_1(\Delta)}(x) dx + b \int_{d_1(\Delta)}^{\infty} (x - z_r) f_{d_1(\Delta)}(x) dx \\ & = h z_r F_{d_1(\Delta)}(z_r) - h \int_0^{z_r} x f_{d_1(\Delta)}(x) dx - b z_r [1 - F_{d_1(\Delta)}(z_r)] + b \int_{d_1(\Delta)}^{\infty} x f_{d_1(\Delta)}(x) dx, \end{aligned} \quad (\text{EC.5})$$

where  $F_{d_1(\Delta)}(x) = \Pr(d_1(\Delta) \leq x)$  and  $f_{d_1(\Delta)}(x)$  is the probability density function of  $d_1(\Delta)$ . Taking the derivative of Eq. (EC.5) with respect to  $z_r$  and evaluating at  $z_r = z_r^*$  yields

$$h F_{d_1(\Delta)}(z_r^*) - b [1 - F_{d_1(\Delta)}(z_r^*)] = 0. \quad (\text{EC.6})$$

The optimal regular target order level is thus given by the critical fractile

$$z_r^*(\Delta) = F_{d_1(\Delta)}^{-1} \left( \frac{b}{b+h} \right). \quad (\text{EC.7})$$

The optimal values  $(z_r^*, \Delta^*)$  of the single index policy are found via the following optimization procedure.

1. Iterate over all values of  $\Delta \in [0, \dots, D_{\max}]$  (or use some search method such as a bisection method), where  $D_{\max}$  is the maximum demand.
2. For each  $\Delta$ , determine the distribution  $F_{d_1(\Delta)}$  for a given  $\Delta$  based on samples of  $D(\Delta)$  that are calculated using Eq. (EC.4).
3. For each  $\Delta$ , calculate  $z_r^*(\Delta)$  according to Eq. (EC.7).
4. Determine the  $(z_r^*, \Delta^*)$  that are associated with the smallest total cost.

## Dual Index

In the dual-index setting (Veeraraghavan and Scheller-Wolf 2008), one keeps track of the regular and expedited inventory positions

$$\tilde{I}_{t+1}^e = \tilde{I}_t^e + q_t^e + q_{t-l}^r - D_t = z_e + O_t - D_t, \quad (\text{EC.8})$$

$$\tilde{I}_{t+1}^r = \tilde{I}_t^r + q_t^e + q_t^r - D_t, \quad (\text{EC.9})$$

where  $l = l_r - l_e$  and  $O_t$  denotes the expedited inventory position overshoot. The dual-index expedited and regular orders are

$$q_t^e = [z_e - \tilde{I}_t^e - q_{t-l}^r]^+, \quad (\text{EC.10})$$

$$q_t^r = z_r - [\tilde{I}_t^r + q_t^e]^+ = D_{t-1} - q_t^e. \quad (\text{EC.11})$$

Similar to the single-index strategy, the inventory evolution can be expressed in terms of target order levels and their difference  $\Delta$ :

$$I_{t+1} = z_e + O_{t-l_e} - \sum_{i=0}^{l_e} D_{t-i} = z_e - d_2(\Delta), \quad (\text{EC.12})$$

where  $d_2(\Delta) = \sum_{i=0}^{l_e} D_{t-i} - O_{t-l_e}(\Delta)$ . Let  $G_{d_2(\Delta)}(x) = \Pr(d_2(\Delta) \leq x)$  denote the cumulative distribution function of  $d_2(\Delta)$ . Similar to single-index policies [Eq. (EC.7)], one determines an optimal expedited target order level according to

$$z_e^*(\Delta) = G_{d_2(\Delta)}^{-1} \left( \frac{b}{b+h} \right). \quad (\text{EC.13})$$

The optimal pair  $(z_e^*, \Delta^*)$  can be found using an iterative search similar to that described in the above single-index policy section. Note that unlike in the single-index policy,  $\Delta^*$  may be larger than the maximum demand  $D_{\max}$ .

## Capped Dual Index

The capped dual index policy (Sun and Van Mieghem 2019) is an extension of the dual index policy and uses the following regular and expedited orders in period  $t$ :

$$q_t^e = [S_t^{e*} - I_t^t]^+ \quad (\text{EC.14})$$

and

$$q_t^r = \min \{ [S_t^{r*} - I_t^{t+l-1}]^+, \bar{q}_t^{r*} \}. \quad (\text{EC.15})$$

Here  $I_t^{t+k}$  are the inventory positions

$$I_t^{t+k} = I_{t-1} + \sum_{i=t-l_e}^{\min(t-l_e+k, t-1)} q_i^e + \sum_{i=t-l_r}^{t-l_r+k} q_i^r, \quad (\text{EC.16})$$

where  $k = 0, \dots, l_r - 1$ . In accordance with Sun and Van Mieghem (2019), we use the convention that  $\sum_{i=a}^b = 0$  if  $a > b$ . The parameters  $(S_t^{r*}, S_t^{e*}, \bar{q}_t^{r*})$  are found via a search procedure. If the demand distribution is time-independent, the CDI parameters are  $S_t^{r*} \equiv S^{r*}$ ,  $S_t^{e*} \equiv S^{e*}$ , and  $\bar{q}_t^{r*} \equiv \bar{q}^{r*}$ .

Without using any search algorithm, the CDI parameters can be estimated according to

$$S_t^{e*} = \frac{h\underline{D}_t^t + b\overline{D}_t^t}{h+b}, S_t^{r*} = \frac{h\underline{D}_t^{t+l} + b\overline{D}_t^{t+l}}{h+b} \quad (\text{EC.17})$$

and

$$\bar{q}_t^{r*} = \frac{h(\underline{D}_t^{t+l} - \underline{D}_t^{t+l-1}) + b(\overline{D}_t^{t+l} - \overline{D}_t^{t+l-1})}{h+b}, \quad (\text{EC.18})$$

where  $\underline{D}_t^n$  and  $\overline{D}_t^n$  denote the minimum and maximum cumulative demand from period  $t$  to  $n$ , respectively (Sun and Van Mieghem 2019).

## Optimal Policy and Value Iteration

Finding an optimal policy that is associated with minimizing the expected cost per period  $J$  [see Eq. (3)] can be obtained via the Bellman equation (Bellman 1954). For a given arbitrary terminal cost function  $v_0(s)$  the update

$$J_{t+1}(s) = \min_{a_t \in \mathcal{A}_t} \left\{ c_t(s_t, a_t) + \gamma \sum_{s' \in \mathcal{S}_t} \Pr(s_{t+1} = s | s'_t, a_t) J_t(s') \right\}, s \in \mathcal{S}. \quad (\text{EC.19})$$

guarantees that  $J^* = \lim_{t \rightarrow \infty} \frac{J_t(s)}{t}$  (Bertsekas 2011). In practice, (EC.19) can be used to solve optimization problems with small state space, and it has been used in the dual sourcing literature as a benchmark of existing methods for small-scale instances (Scheller-Wolf et al. 2007).

Before describing the value iteration implementation, we state two simplifications that can be done without loss of generality. First, the lead time and the unit ordering cost of the expedited supplier can be set to zero:  $l_e = c_r = 0$  (Sheopuri et al. 2010, Sun and Van Mieghem 2019). Second, the dimensionality of the state space can be compressed to  $l$  components (Sheopuri et al. 2010). We can define the expedited inventory position  $\tilde{I}_t^e = I_t + q_{t-l}^r$  and compress the state vector to  $s_t = (\tilde{I}_t^e, q_{t-l+1}^r, \dots, q_{t-1}^r)$ .

Once actions  $(q_t^r, q_t^e)$  have been taken and demand  $D_t$  is realized, the period cost is calculated as  $f(\tilde{I}_t^e + q_t^e - D_t)$ , where  $f(x) = hx^+ + b[-x]^+$ . For convenience, we define  $Q = (q^r, q^e)$  and  $\mathcal{D}_Q$  the domain of optimal actions. The state update equations become

$$\begin{cases} \tilde{I}_{t+1}^e \leftarrow \tilde{I}_t^e + q_t^e + q_{t-l+1}^r - D_t \\ q_{t-l+1}^r \leftarrow q_{t-l+2}^r \\ \dots \\ q_{t-1}^r \leftarrow q_{t-2}^r \end{cases} \quad (\text{EC.20})$$

The value iteration algorithm then proceeds as follows.

- For each state  $s \in \mathcal{S}$ , select an arbitrary initial cost  $J_0(s)$
- For a given state  $s$  and action  $Q$ , find the transition probabilities to state  $s'$  according to the demand distribution  $\phi$ . Let us denote those probabilities by  $P(s'|s, Q)$ . Calculate the cost  $f(s')$  associated with each transition  $s \xrightarrow{Q} s'$ . Iterate those calculations for all combinations  $(s, Q) \in \mathcal{S} \times \mathcal{D}_Q$ .

- Apply the update  $J_{k+1}(s) = \min_{Q \in \mathcal{D}_Q} \left\{ c^e q^e + \sum_{s' \in \mathcal{S}} P(s'|s, Q)(f(s') + J_k(s)) \right\}$ , for all  $s \in \mathcal{S}$
- Calculate the average cost approximation  $\lambda_{k+1}(s) = J_{k+1}(s)/(k+1)$ , for all  $s \in \mathcal{S}$
- Iterate the above update until  $\max_{s \in \mathcal{S}} \{\lambda_{k+1}(s) - \lambda_k(s)\} < \epsilon$

## Neural-network Structure and Learning Characteristics

To provide insights into the representational capacity and learning characteristics of IDINNs, we briefly discuss properties of (i) network structure as the basis of the potential representational power of a neural network, and (ii) learning dynamics and optimizers that help to learn effective inventory management policies.

The network structure that we employ in dual-sourcing problems with demand distribution  $\mathcal{U}\{0, 4\}$  uses the  $(l_r + l_e + 1)$ -dimensional state  $s_t = (I_{t-1}, Q_{t-1}^r, Q_{t-1}^e)$  as an input and outputs actions  $\hat{a}_t = (\hat{q}_t^r, \hat{q}_t^e)$ . As hidden layers, we use fully connected layers with CELU activation that resemble the  $\max(\cdot)$  operations inventory management heuristics (see Sec. 2.1). CELU activations (9) approximate ReLU activations in the limit  $\alpha \rightarrow 0$ . In all numerical experiments, we use seven hidden layers with 128, 64, 32, 16, 8, 4, and 2 neurons, respectively. We set  $\alpha = 1$ .

Hanin and Sellke (2017) and Park et al. (2020) formulated a universal approximation theorem and width bounds for neural networks with ReLU activations. In particular, they derived the conditions under which neural networks with ReLU activations can approximate any continuous, real-valued function arbitrarily well. These theorems supported our choice to use a neural network with CELU activations. Finally, (C)ELU activations are continuously differentiable and thus facilitate faster learning via gradient backpropagation without using unit natural gradients near 0 activations (Clevert et al. 2015).

We train neural networks using inventory time series with  $T = 100$  ( $l_r = 2$ ), 150 ( $l_r = 3$ ), and 200 ( $l_r = 4$ ) periods and minibatches of size 512. Large minibatch sizes and sufficiently long time series help to appropriately sample the action space. The use of large enough minibatches also aligns gradient descent in the direction of the global optimum (Li et al. 2014, Masters and Luschi 2018). The employed optimizer, RMSprop (see Eq. (5)), is an adaptive learning rate method that is well-suited to perform mini-batch weights updates. For most parts of the learning process, we use a learning rate of  $3 \times 10^{-3}$  for the neural-network parameters and a learning rate of  $10^{-1}$  for the adjustment of the initial net inventory. Adjusting the initial inventory during the learning process is helpful for IDINNs to identify efficient policies on finite time horizons. As IDINN-based policies approach optimal policies, it may help to lower the learning rates by up to an order of magnitude.

As detailed in the main text, standard backpropagation methods rely on real-valued gradients and neural-network parameters. To generate discrete actions (*i.e.*, order quantities in inventory management problems), we decouple the fractional part of an action before generating the corresponding output as described in (Asikis 2021).

To train IDINNs to manage dual-sourcing problems with empirical demand data, we use as inputs in the first layer of the neural network the mean  $\mu_t$  and standard deviation  $\sigma_t$  of the truncated normal distribution (17), and the reduced state  $(I_t + q_{t-1}^r, \tilde{Q}_t^r, Q_t^e)$ , where  $\tilde{Q}_t^r = (q_{t-l_r}^r, \dots, q_{t-2}^r)$ .

The input state is therefore  $(l_r + l_e + 2)$ -dimensional. The hidden layer consists of 3 linear layers with 6 CELU activations each. Building on ideas from computer vision (Fei-Fei et al. 2006), we employ a “one-shot learning” protocol where we pretrain the neural network on one specific demand realization. The learning rate was initially varied between  $1 \times 10^{-3}$  and  $3 \times 10^{-3}$ , and then reduced to  $2 \times 10^{-4}$  after reaching an average cost per period of  $8 \times 10^5$ . In the second step, we trained the IDINN on 4 samples to improve performance. Learning rates varied between  $1 \times 10^{-4}$  and  $3 \times 10^{-3}$ . The total training time is between 20 minutes and about 1 hour on an Intel<sup>®</sup> Core<sup>™</sup> i7-10510U CPU @ 1.80GHz.

## Acknowledgments

LB acknowledges financial support from the Swiss National Fund (P2EZIP2.191888).